UNITED NATIONS UNIVERSITY
UNU-GTP
Geothermal Training Programme

Orkustofnun, Grensasvegur 9,
IS-108 Reykjavik, Iceland

Reports 2015
Number 32

SEISMIC MONITORING OF GEOTHERMAL FIELDS: A CASE STUDY OF HELLISHEIDI GEOTHERMAL FIELD

Shashika Amali Samaranayake
National Institute of Fundamental Studies
Hantana road, Kandy
SRI LANKA
samaranayakerusl@gmail.com

ABSTRACT

The study of induced seismicity in geothermal fields can be used to understand the physics of the ongoing processes in the reservoir. Microseismic activity in reservoirs can result from brittle deformation of reservoir rocks due to mass extraction and reinjection. Careful installation of monitoring stations is the initial step of all monitoring procedures. Information gained from seismic monitoring forms the basis of mitigating risk associated with induced seismicity. Mitigation procedures can be divided into three steps: understanding the background seismicity to identify whether events are natural or induced; install a permanent, stand-alone surface-based seismic network; and implement risk management procedures.

Seismic activity connected with reinjection of waste water at the Hellisheidi power plant is considered for this case study, and the seismic events recorded during a seismic swarm in 21 -22 April 2012 are analysed. Successful methodologies and processing methods that can be used to monitor geothermal field are discussed and compared with global scenarios.

1. INTRODUCTION

Geophysics is a branch of physics and one of the most powerful ways to explore the interior of the earth. It is an interdisciplinary science composed of physical principles that allow us to determine the physical contrast of formations and processes in the deep via remote sensing manners. Geophysics integrate the observations, hypotheses and theories of geology with the techniques and principles of physics to understand the composition, nature, structure and processes of the earth. There are many methods involved in geophysical exploration and the techniques differ with the objective.

Geophysical methods are widely used in geothermal resource exploration and monitoring. It provides basic information about the reservoir and necessary information to demarcate the resource periphery. Magnetotellurics (MT), Time Domain Electromagnetics (TDEM), gravity and magnetic techniques are prominent in geothermal exploration and seismic methods are mostly involved in the monitoring stage. Large scale mass extraction for a long time period can lead to internal changes of the subsurface and continuous monitoring of the reservoirs and its vicinity becomes inevitable (Evans et al., 2011). Fluid re-injection has been introduced for mass balancing, preventing possible subsidence at extraction sites

and recharging the geothermal system (Halldórsson et al., 2012). These measures can induce or trigger microseismic activity at the geothermal sites, causing concern among people living in the vicinity.

Nowadays, studies on induced seismicity are one of the major topics in the geothermal field because of the public concerns (Halldórsson et al., 2012). Induced seismicity can be defined as earthquake activity resulting from human activity that causes a rate of energy release, or seismicity recorded beyond its normal level. A number of activities can cause induced seismicity. It is common in relation with production in geothermal fields, in connection with reservoir impoundment, waste injection and oil and gas exploration. The seismicity is thought to take place when the effective stress is decreased so that the rock can no longer withhold the stress and it is released in an earthquake. The effective stress can either be reduced by increasing the pore pressure or decreasing the surrounding stress. Hydraulic fracturing is also associated with induced seismicity. In that case water is injected into the sub surface under high pressure, creating new fractures effectively linking existing fractures together. This activity creates additional permeability in the subsurface (LBNL, 2015).

There are global examples where public objections against induced seismicity have either delayed, altered or altogether cancelled proposed geothermal projects (Evans et al., 2011). Therefore, induced seismicity is an important and practical issue that should be handled very carefully when developing geothermal projects (Halldórsson et al., 2012). Icelandic induced seismic activities are not normally considered as risk elements and are focused on widening the micro fractures to enhance the effective permeability (Gunnarsson et al., 2015). Continuous and thorough monitoring of seismicity assists in making decisions, in order to avoid negative side-effects and possible risks on the community due to induced seismicity. It is important to follow an appropriate methodology to obtain a clear picture of subsurface processes. The methodology proposed here is location specific, yet with common features and infrastructure that can be applied in any area.

2. OBJECTIVE

Detecting underground fractures is very important for geothermal reservoir exploration and micro earthquakes are very good indications for the existence of such fractures. Many developing geothermal fields maintain a small earthquake monitoring system, but the systems are not fully used for geothermal exploration. The main objective of this study is to discuss the procedures of installing, maintaining, acquiring and processing seismic data for sustainable maintenance of geothermal resources. A case study was done in the Húsmúli area in Iceland which relates to one of Iceland´s largest high-temperature geothermal fields and the largest power plant.

3. BACKGROUND OF CASE STUDY AREA

The Hellisheidi field is located in the southern part of the Hengill volcanic system and is a naturally seismic area. The area is characterized by NE-SW oriented fissure swarms and hyaloclastite formations as shown in Figure 1. The geothermal system in Hellisheidi is located in fractured bedrock. The Hellisheidi power plant started operations in 2006 and has a 303 MWe installed electrical capacity and a thermal capacity of 133 MWth, which is utilized for district heating. The major challenge of the power plant operation is re-injection, since injecting all the brine into the geothermal reservoir is a primary requirement and a legal obligation. This is quite difficult because of the temperature dependant performance of the injection wells and the increased level of seismicity immediately following the start of re-injection. (Gunnarsson, 2013). Hellisheidi power plant has two re-injection zones. The previous zone was at Gráuhnúkar, situated on the southern edge of the Hellisheidi geothermal field. Gráuhnúkar has a very high formation temperature and it has been suggested as a possible production zone. The current injection site is at Húsmúli at the northern edge of the field. It has a comparably low formation

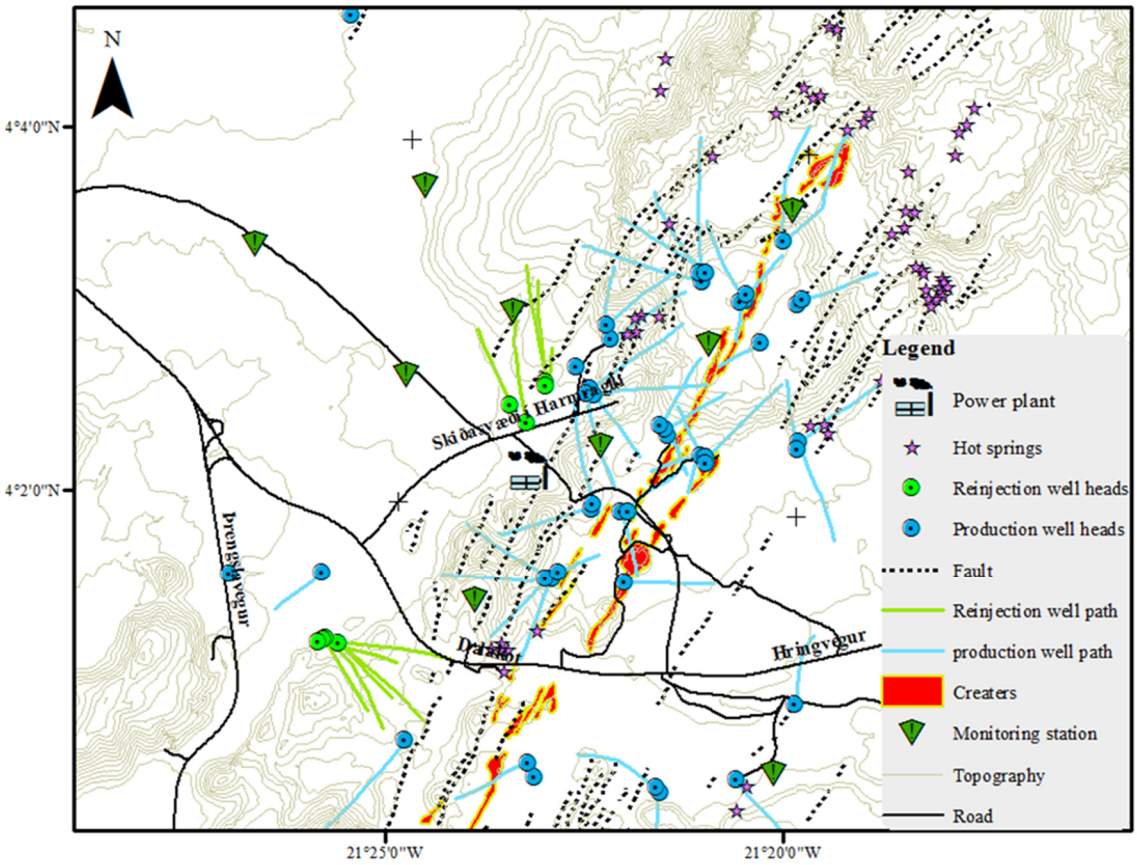

FIGURE 1: Topographical map of the Hellisheidi geothermal field with related faults, craters, surface manifestations, production wells, injection wells and seismic monitoring stations

temperature and the zone re-injectivity depends on the re-injection temperature. The injectivity at Húsmúli is higher for cold water, which can be explained by the changing aperture of fractures due to thermal expansion and contraction, which has a major effect on permeability and outweighs the effects of viscosity. It can be described simply as fracture-dominated permeability. Seven wells have been drilled in the Húsmúli zone. Five directional wells are used as re-injection wells, one is impermeable and one shallow well is used as an observation well. The drilling targets of the Húsmúli re-injection wells are the fault zones associated with the Húsmúli area. Re-injection was started in September 2011 and was followed by a swarm of induced seismicity culminating in two ~4.0 M events on October 15th, 2011 (Gunnarsson et al., 2015). This was an unexpected situation but as proposed the seismicity gradually decreased with continued operations. The decrease of seismic activity with time can be explained by the release of natural stress built up in the crust due to crustal movements.

Most mapped faults in the Hengill formation follow a NE-SW direction and are normal faults. There are some N-S trending faults recorded in post seismic monitoring and it has been suggested that there is a relationship between those faults and the South Iceland Seismic Zone (SISZ). N-S trending faults with a strike-slip behaviour are a typical feature of the SISZ (Gunnarsson et al., 2015) and the Hengill formation marks the western boundary of the SISZ.

A local seismic network was operated in the Hengill area by Uppsala University, MIT and ISOR during the induced seismic activities following the reinjection in Húsmúli. It was a part of a larger network operated from 2009 to 2013 ranging from the western part of the Reykjanes Peninsula to the eastern part of the Hengill volcanic system. Currently the closest station is ~10 km away. It is a part the Icelandic Meteorological Office's regional network.

4. THEORY

4.1 Elasticity and seismic wave

Earthquake seismology is a subject that evaluates ground motion produced by an energy source within the earth. In this case it is assumed that the ground returns to its initial position except at the vicinity of the source. This type of vibrations leads to small scale elastic deformations or strains in response to the initial forces in the rock or *stresses*. Using the theory of elasticity, we can explain the behaviour of earthquake waves mathematically. Energy that originates from an earthquake travels through the medium as different kinds of waves, mainly as body waves and surface waves. There are two kinds of body waves, called P waves and S waves. P waves involve compressional motion and volumetric changes as the wave disturbances passes through the continuum. S waves involve shearing motions without volume change (see Figure 2).

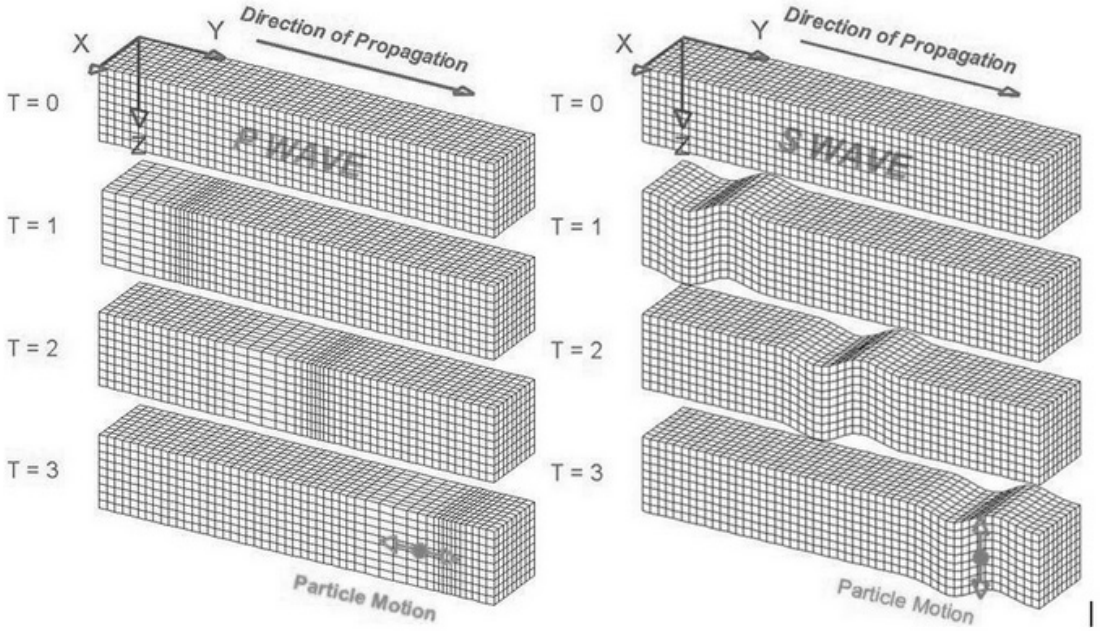

FIGURE 2: P and S wave propagation. (Seale et al., 2011)

Helmholtz's theorem can be used to derive mathematical equations for P and S waves. It states that any vector field $\boldsymbol{U}$ can be represented in terms of a vector potential $\boldsymbol{\Psi}$ and a scalar potential ϕ by,

$$\boldsymbol{U} = \boldsymbol{\nabla}\phi + \boldsymbol{\nabla} \times \boldsymbol{\Psi} \tag{1}$$

where $\boldsymbol{\nabla} \cdot \phi$ = Curl free scalar potential field $(\boldsymbol{\nabla} \times \phi = 0)$ for non-shearing motion; and
$\boldsymbol{\nabla} \times \boldsymbol{\Psi}$ = Divergence less vector potential field $(\boldsymbol{\nabla} \cdot \boldsymbol{\Psi} = \boldsymbol{0})$ involves no changes in volume.

Equation of a motion gives force balance on a cubic element in a continuum that is undergoing internal motions:

$$\rho\left(\frac{\partial^2 u_i}{\partial t^2}\right) = f_i + \frac{\partial \sigma_{ij}}{\partial x_j} \tag{2}$$

where, ρ = Density of the continuum;
u = Displacement;
f_i = Component of body force per unit volume;
σ_{ij} = Stress component;
i - Corresponds to the direction normal to the plane being acted on force;

j - Direction of the force.

When no body-forces are considered, we get the homogeneous equation of motion as follows:

$$\rho\left(\frac{\partial^2 u_i}{\partial t^2}\right) = \frac{\partial \sigma_{ij}}{\partial x_j} \tag{3}$$

The most general form of a constitutive law for linear elasticity is Hooke's law. It states that the stress and strain are linearly related and is given by:

$$\sigma_{ij} = C_{ijkl}\varepsilon_{kl} \tag{4}$$

where C_{ijkl} = Elastic moduli defining the material properties of the medium;
ε_{kl} = Strain tensor.

The elastic properties for many materials and material composites in the Earth are independent of direction or orientation of the sample. Isotropic elastic substances have only two independent elastic moduli called the Lamé constants, λ and μ. The relationship between those and Hooke's law is given by:

$$\sigma_{ii} = \lambda\theta + 2\mu\varepsilon_{ii} \text{ (Figure 3)}$$
$$\sigma_{ij} = 2\mu\varepsilon_{ij} \tag{5}$$

where θ = Trace of the strain tensor:$\left(\frac{\partial u_1}{\partial x_1} + \frac{\partial u_2}{\partial x_2} + \frac{\partial u_3}{\partial 3}\right)$.

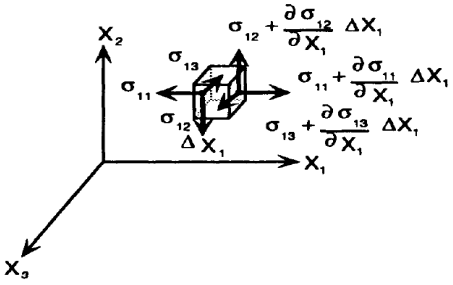

FIGURE 3: A cubic element in the continuum bounded by faces paralleling the coordinate planes. Balancing the stresses on each face acting in a given direction leads to the equation of equilibrium. Only the stresses acting on $\pm x_1$ face are shown. Similar stress terms act on the other four faces (Lay and Wallace, 1995)

This relationship gives following statements (Equation 6):

$$\sigma_{11} = \lambda\left(\frac{\partial u_1}{\partial x_1} + \frac{\partial u_2}{\partial x_2} + \frac{\partial u_3}{\partial 3}\right) + 2\mu\frac{\partial u_1}{\partial x_1}$$

$$\sigma_{12} = 2\mu\varepsilon_{12} = \mu\left(\frac{\partial u_1}{\partial x_2} + \frac{\partial u_2}{\partial x_1}\right) \tag{6A}$$

$$\sigma_{13} = \mu\left(\frac{\partial u_1}{\partial x_3} + \frac{\partial u_3}{\partial x_1}\right)$$

where angular distortion between segments in the x_1 and x_2 directions gave:

$$\varepsilon_{12} = \frac{1}{2}\left(\frac{\partial u_1}{\partial x_2} + \frac{\partial u_2}{\partial x_1}\right) \tag{6B}$$

Using the above relationships in Equation 3 we can rewrite things as follows:

$$\rho\left(\frac{\partial^2 u_i}{\partial t^2}\right) = \lambda\frac{\partial\theta}{\partial x_i} + \mu\frac{\partial}{\partial x_i}\left(\frac{\partial u_1}{\partial x_1} + \frac{\partial u_2}{\partial x_2} + \frac{\partial u_3}{\partial x_3}\right) + \mu\left(\frac{\partial^2 u_i}{\partial x_1^2} + \frac{\partial^2 u_i}{\partial x_2^2} + \frac{\partial^2 u_i}{\partial x_3^2}\right) \text{ or}$$
$$\rho\left(\frac{\partial^2 u_i}{\partial t^2}\right) = (\lambda + \mu)\frac{\partial\theta}{\partial x_i} + \mu\nabla^2 u_i \tag{7}$$

We can write all three components of above equations in the equivalent vector format as follows:

$$\rho\ddot{\boldsymbol{u}} = (\lambda + \mu)\boldsymbol{\nabla}(\boldsymbol{\nabla}\cdot\boldsymbol{u}) + \mu\nabla^2\boldsymbol{u} \tag{8}$$

Using the vector identity:

$$\nabla^2 \boldsymbol{u} = \boldsymbol{\nabla}(\boldsymbol{\nabla} \cdot \boldsymbol{u}) - (\boldsymbol{\nabla} \times \boldsymbol{\nabla} \times \boldsymbol{u}) \tag{9}$$

we can rewrite Equation 8 as follows:

$$\rho \ddot{\boldsymbol{u}} = (\lambda + 2\mu)\boldsymbol{\nabla}(\boldsymbol{\nabla} \cdot \boldsymbol{u}) - (\mu \boldsymbol{\nabla} \times \boldsymbol{\nabla} \times \boldsymbol{u}) \tag{10}$$

Substituting Equation 1 in to Equation 10, we get;

$$\boldsymbol{\nabla} \underbrace{\left[(\lambda + 2\mu)\nabla^2 \phi - \rho \ddot{\phi}\right]}_{0} + \boldsymbol{\nabla} \times \underbrace{\left[\mu \nabla^2 \boldsymbol{\Psi} - \rho \ddot{\boldsymbol{\Psi}}\right]}_{0} = \boldsymbol{0} \tag{11}$$

which can be satisfied if each term in the brackets goes to zero as indicated:

$$\begin{aligned} &\textbf{(i)} \quad \left[(\lambda + 2\mu)\nabla^2 \phi - \rho \ddot{\phi}\right] = 0; \text{ Scalar wave equation} \\ &\nabla^2 \phi - \frac{1}{\alpha^2} \ddot{\phi} = 0; \alpha = \sqrt{\frac{\lambda + 2\mu}{\rho}} \text{ (P wave velocity)} \\ &\textbf{(ii)} \quad \left[\mu \nabla^2 \boldsymbol{\Psi} - \rho \ddot{\boldsymbol{\Psi}}\right] = 0; \text{ Vector wave equation} \\ &\nabla^2 \boldsymbol{\Psi} - \frac{1}{\beta^2} \ddot{\boldsymbol{\Psi}} = 0; \beta = \sqrt{\frac{\mu}{\rho}} \text{ (S wave velocity)} \end{aligned} \tag{12}$$

For most materials both λ and μ are positive, therefore α is always higher than β and the P wave is always the first wave arriving from an earthquake.

4.2 Data processing

The primary objective of observational seismology is to locate seismic sources. The hypocentre and the source origin-time are the parameters which need to be solved for in seismic processing. The major factors that are required to determine the origin of an earthquake are the identification of seismic phases, measuring their travel time, and the velocity structure between source and seismic station. Both forward and inverse modelling can be used to solve the seismic problem addressing the above parameters (see Figure 4). Inverse modelling is the most used method for processing seismic data as well as other geophysical data.

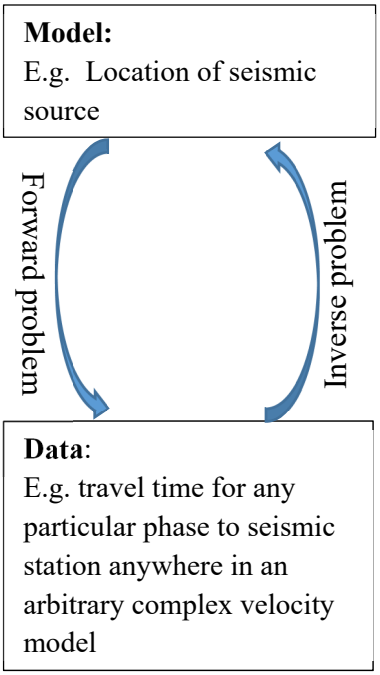

FIGURE 4: Forward and inverse problem

4.2.1 Forward algorithm

The number of stations that collect raw data for an event is a crucial factor to locate seismic activity accurately. In theory, even a single station is adequate to locate an earthquake, however, practically only a very crude estimation can be obtained. When several stations are available, an accurate location can be determined by using P and/or S wave arrival times. If the event is local, close to the stations, the two principle phases on the seismogram are P and S. The Wadati diagram is a technique that is used to find the origin time of the earthquake (Figure 5). In this case, time difference between S and P waves (t_s-t_p) are plotted against the absolute arrival time of the P wave. Since (t_s-t_p) goes to zero at the hypocentre, a straight line fit on Wadati diagram provides an approximate origin time (T_{origin}) of the event (Lay and Wallace, 1995).

4.2.2 Calculation of epicentre of the event by graphical method

It is possible to calculate the P wave travel time by using T_{origin} and the P travel time of the ith station. By using the P wave travel time and the P wave velocity (α), the epicentral distance for the ith station (D_i) can be easily calculated.

$$D_{focal} = \sqrt{D_i^2 - D_{prop.}^2} \tag{13}$$

A possible location of the earthquake lies on the circumference of circle with the radius D_i. The epicentre should be located at the intersection of circles drawn for each station. The focal depth $D_{focal,}$ according to the ith station, can be determined by Equation 13, where $D_{prop.}$ is the distance along the surface to the epicentre.

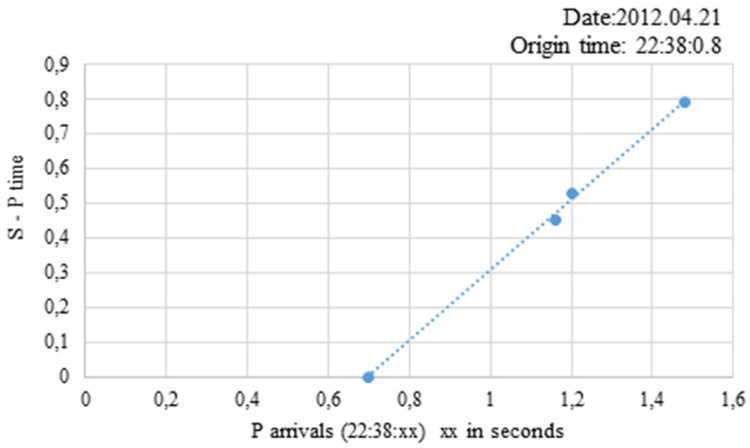

FIGURE 5: An example of the Wadati diagram method for determining the origin time. The intersection with the P wave arrival time axis gives the origin time (event related in case study site)

More observations always make complications, since they give more intersections. Our primary target is to determine four unknowns: X, Y, Z and origin time. We can assume a solution and calculate expected P-wave arrival times. Comparing this prediction with the real observation, the difference between calculated and observed arrival times can be determined. Shifting predicted parameters according to the deviations, a new model can be recalculated with an improvement. The procedure continues until an acceptable difference between calculated and observed arrivals are obtained. This is the procedure of forward modelling.

4.2.3 Inverse modelling

The model data that is approximately similar to the observed data can be mathematically described as follows. Introduce function *f*, which calculates the arrival time as a function of location (x_i, y_i, z_i) and velocity (v):

$$t_{i(predicted)} = f(x_i, y_i, z_i, v) = t_{i(observed)} \tag{14}$$

If we have n number of stations, our data (observation) vector is $\boldsymbol{d} = (t_1, t_2, \dots, t_i, \dots, t_n)$ where t_i is observed P arrival time on the ith station. The model parameters come in vector $\boldsymbol{m}$ and it has four components for location and origin time:

$$\boldsymbol{m} = \left(x, y, z, t_{i(predicted)}\right) \tag{15}$$

$$\overline{\boldsymbol{F}}(\boldsymbol{m}) = \boldsymbol{d} \tag{16}$$

$\overline{\boldsymbol{F}}$ is a matrix called the data kernel.

If we can divide $\overline{\boldsymbol{F}}(\boldsymbol{m}) = \boldsymbol{d}$, by some operator $\overline{\boldsymbol{F}}^{-1}$ to give $\boldsymbol{m}$ directly, we are solving the problem inversely. In a homogeneous half space, consider the Cartesian coordinates of the true hypocentre (x, y, z) and the coordinates of the ith station (x_i, y_i, z_i). Then the arrival time of the ith station can be written as follows:

$$t_i = t_{origin} + \frac{\sqrt{(x_i - x)^2 + (y_i - y)^2 + (z_i - z)^2}}{v} \quad (17)$$

where t_i = Arrival time of the i[th] station;
v = Velocity.

Ideally, only one unique set of parameters fits with the observed values. According to $\overline{\boldsymbol{F}}(\boldsymbol{m}) = \boldsymbol{d}$, we can write $\overline{\boldsymbol{F}}(x, y, z, t) = \boldsymbol{d}$. The equation for $\boldsymbol{d}$ is nonlinear, so we must linearize the problem and iteratively improve the solution (model parameters). This can be done with a Taylor series approximation. This links the needed changes in hypocentral location with the difference in observed and predicted travel time. We define the partial derivative matrix of our problem as G_{ij} with respect to the i^{th} station's j^{th} model parameter as:

$$G_{ij} = \frac{\partial d_i}{\partial m_j} \quad (18)$$

Then we can rewrite our problem as $\Delta\boldsymbol{d} = \boldsymbol{G}\Delta\boldsymbol{m}$ or $\boldsymbol{d} = \boldsymbol{G}\boldsymbol{m}$. This is the linearized form of the problem. If we have 4 stations we have $\boldsymbol{n}=\boldsymbol{m}$ type problem and Gaussian elimination can be used to solve it. Once $\delta x, \delta y, \delta z$ and δt are calculated, we can modify the parameters using the equation $m_j^1 = m_j^0 + \delta m_j^0$. This iterative process can be continued until $\Delta\boldsymbol{d}$ becomes acceptably small. This method is known as Geiger's method. Its disadvantages are that the final model totally depends on the initial guess and the process does not guarantee convergence (Lay and Wallace, 1995).

$\boldsymbol{d} = \boldsymbol{G}\boldsymbol{m}$ gives $\boldsymbol{G}^{-1}\boldsymbol{d} = \boldsymbol{m}$.

Solution of this equation is quite easy. However, as seismology data has several errors and the velocity model can be changed, it means the equations are inconsistent making it impossible for us to use this simple equation. With many observations ($\boldsymbol{n}>\boldsymbol{m}$), as in the case of earthquake location problems, we can obtain an overdetermined solution, which is the best fit to an average of the data.

4.3 Theory of induced seismicity

Induced seismicity is earthquake activity resulting from human activity that causes an increased rate of energy release, or seismicity, which exceeds the normal level of background seismic activity. In order to discern the induced seismicity from the natural seismicity, surveys of the regional background activity should be conducted before operations are started. Berlin in El Salvador, is a good example of a geothermal field with high levels of recorded background seismicity (Majer et al., 2007).

Induced seismicity has been recorded in a number of operating geothermal fields worldwide. In most of these cases thousands of small events have been recorded annually (Majer et al., 2007). Drilling, mass extraction and reinjection are all capable of inducing seismicity in the related area. Notable cases are: Rangely, CO, injection experiments (M4.9, 1995), 1945-1995; Rocky Mountain Arsenal (M5.3, 1967), fluid injection; Gazli, Uzbekistan, gas recovery (M7.2), 1976-1984; Lake Mead (M5), reservoir impoundment; Geysers geothermal field (M4.6), injection-enhanced production; Youngstown, Ohio (M4.0), fluid injection, 2011. It is important to identify the causes of the induced seismicity to be able to take precautions for the future sustainability of the project.

There are several different mechanisms that have been proposed to explain the occurrence of induced seismicity in geothermal areas (See Figure 6). Stress is the major factor that affects induced seismicity. Some of the major mechanisms of induced seismicity in geothermal environments are categorized as follows (Majer et al., 2007):

1. Pore pressure increase

Increased fluid pressure can decrease static friction and facilitate seismic slip in the presence of a deviatoric stress field. Sometimes seismicity is driven by the local stress field, but triggered on an

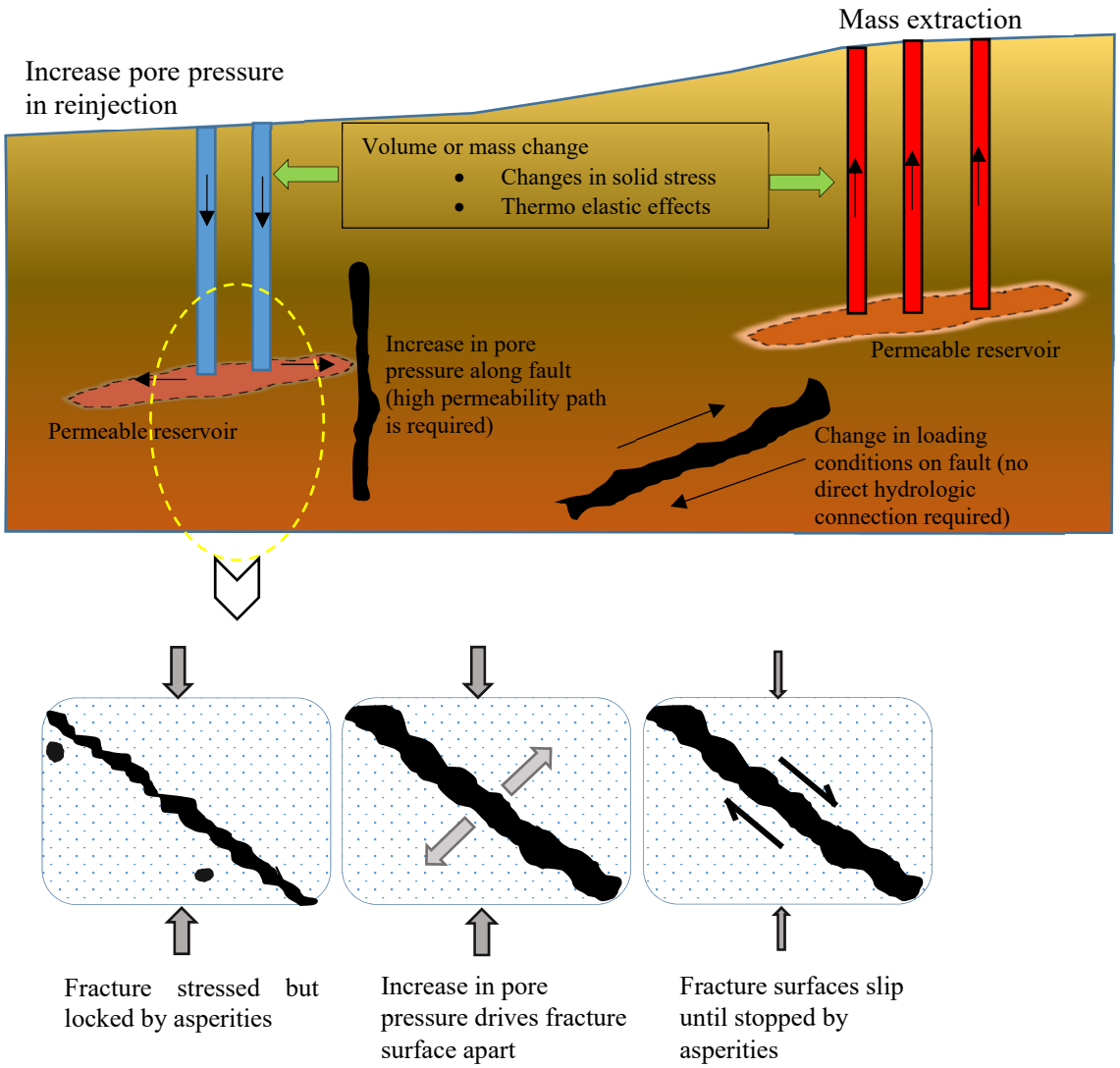

FIGURE 6: Earthquake course explained by mass extraction and re injection (after Nordquist (2005) and Ellsworth (2013))

existing fracture by increasing pore pressure. The pore pressure increase required can in some cases be very low. Many seismic events occur as the pressure migrates away from the wellbore in the direction of principle stress. Fluid injection in geothermal fields obviously increases the pore pressure in that area, resulting in high seismic activity around the injection well, provided that there are local regions of low permeability. High-pressure fluid injection can exceed the rock strength and create new fractures in the rocks (Majer et al., 2007).

2. Temperature decrease

When cool fluid is injected into the sub surface it interacts with the hot rock which can cause contraction of the fracture surface. Cool fluid and hot rock interaction can also create fractures and seismicity directly with the thermal contraction (Majer et al., 2007).

3. Volume change due to mass extraction and reinjection

Fluid level changes (reduction or increase) will affect the reservoir rock. It can compact or be stressed. The volume changes cause a perturbation in the local stress conditions, which can lead to a slip on a fault that is close to failure. This is common in geothermal fields as they are often situated within faulted regions under high stress, and will cause a seismic slip within or around the reservoir (Majer et al.,2007).

4. Chemical alteration of fracture surfaces

Injecting non-native fluid can change the chemical composition in the reinjection area. It may cause geochemical alteration of fracture surfaces and cause a change in the coefficient of friction on those surfaces (Majer et al., 2007). One or more of the phenomenon mentioned above can be involved in the onset of earthquakes.

5. METHODOLOGY

5.1 Seismographs

Seismographs are generally composed of two major components: A sensor to measure the ground motion, known as a seismometer, and a recording system. Most seismometers are three-component devices that measure the ground motion along three orthogonal directions. These components are normally aligned to N-S, E-W (horizontal plane) and vertical directions. Modern seismometers can be categorized according to their dynamic range. *Long period seismometers* record very low frequencies and are usually designed to measure seismic signals with frequencies in the range 0.01 Hz - 0.10 Hz. *Short period seismometers* have a very short natural period and a correspondingly high resonant frequency which is higher than most frequencies of a seismic wave. They are usually designed to respond to frequencies in the range of 1 Hz-10 Hz. *Broadband seismometers* are highly sensitive over a wide range, typically between 0.1 Hz and 50 Hz.

Selecting a proper frequency range is very important for successful data gathering and achieving objective(s). In geothermal monitoring, the expected signal has a high frequency. Therefore, seismometers with dynamic range of 1-10 Hz (short period seismometers) are in order. To be able to detect the low magnitude events some magnification might be necessary in the digitizer (recording system).

5.2 Deployment of seismometers

When deploying seismic stations, we must consider the number of required stations, distance to expected activity and coverage angle of the network. The deployment has to be thoroughly planned to ensure the detection of possible unrest due to geothermal related activities. The geology of the area is one of the prime concerns in selecting locations for seismometers in close proximity to the production and re-injection wells. During the drilling period additional seismic stations may add to the system to detect possible induced seismicity changes due to drilling operations. Before deploying the seismometer, we should have a good idea of the target event area. Figure 7 shows a seismometer network and two seismic events, A and B. Both events are covered by the same number of stations. However, event B is detected by stations covering a 360° angle around the event while event A is only covered by stations on one side. Azimuthal coverage greatly influences the location accuracy of seismic events. Installing a station close to the epicentre can greatly improve the determination of depth.

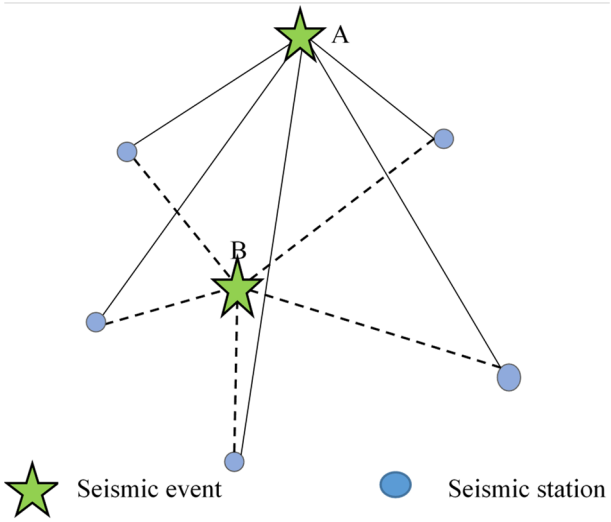

FIGURE 7: Simulated seismic array for detecting earthquakes

5.3 Installation of a seismic station

The classification of seismometers additionally depends on the environment in which they are deployed. Two major types of classifications are inland and ocean bottom seismometers. The installation procedures of these two types are quite different.

5.3.1 Inland seismometer

Inland seismometers are the most available type and simpler to deploy. They can either be a part of a real time monitoring system or a post processing system. Initial procedures are identical for the two systems and additional components are added to the real time monitoring system. Environmental factors are of great importance in the installation of a seismic station. The sensor needs to be well protected from environmental noise, such as temperature fluctuation, turbulent air flow around walls and human activity. This can be done by selecting a suitable site, and placing the sensor in a protective enclosure. For the best possible results, a seismometer should be installed in a specially built vault, where conditions are near perfect. Different kinds of techniques are used to achieve this near perfect status. Some of them are:

- Standing the sensor on a concrete cylinder which is perfectly coupled to solid bed rock;
- Use only a little extra mass to create the concrete cylinder;
- Use rock wool or other insulators for insulation;
- Shield from wind and rain;
- Isolate area from human activity etc.;
- Suitable distance from sensor to mast;
- Clearing the floor of the hole of all loose material.

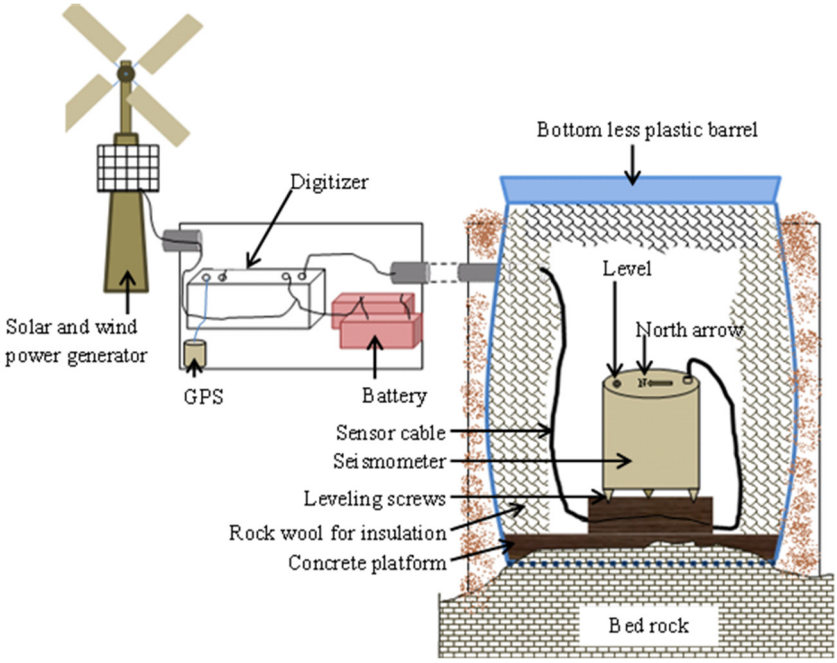

FIGURE 8: Schematic diagram of an inland seismometer

The setup of a protective enclosure is the first step of installation, as described in Figure 8, as well as the whole system of an inland seismic station.

There are two factors that need to be considered when a sensor is installed in the protective enclosure: 1) align the sensor to true north, and 2) level the sensor. Optimally we should use a gyro compass to find true north, because it is not affected by the surrounding rock's magnetic properties (Figure 9). It is convenient to draw the N-S line in the surface of the concrete cylinder. Before placing the sensor on the line it is recommended to connect the cable, because once the sensor is

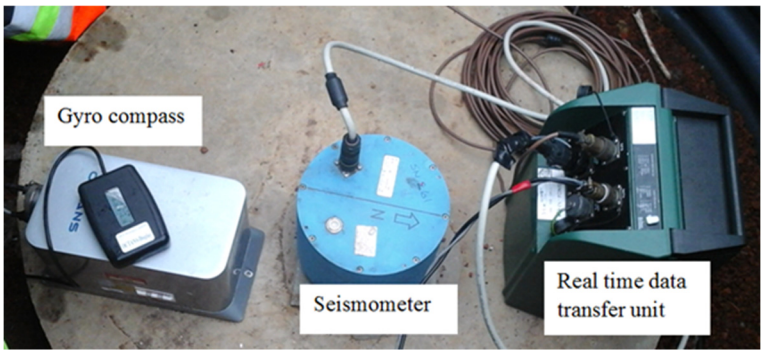

FIGURE 9: Setup of a gyro compass survey at Reykjanes peninsula

properly aligned, connecting cables may disrupt the sensor position. Then the sensor is placed on the line to align the sensor to the true north direction. To facilitate this, sensors often have a steel pointer on the instrument which shows the north axis of the sensor. Then the sensor is levelled by adjusting each of the three screws on the bottom of the instrument, until the bubble in the spirit level lies entirely within the inner circle (Figure 10). As the final step, the sensor is connected to the seismic recording system. There are different types of energy sources used for seismic stations, such as battery, solar power, wind power etc. In post processing systems, data is recorded on flash memory cards which are collected routinely. Real time monitoring systems data recorders are linked to a communication tower which transmits directly to the working station.

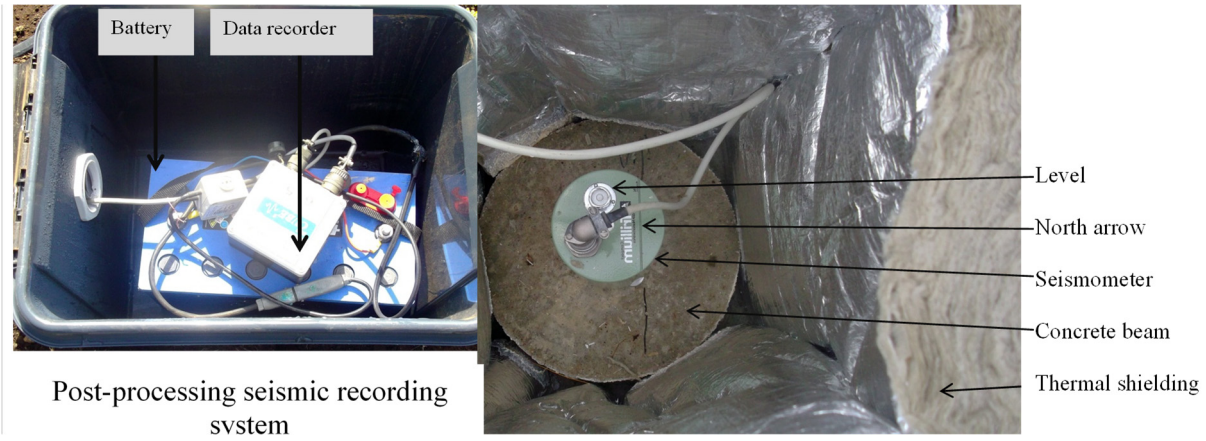

FIGURE 10: Parts of the seismic monitoring stations

5.3.2 Ocean bottom seismometers (OBS)

This is not a prominent method in geothermal projects; because most geothermal projects are away from the ocean and deploying procedures are very complicated. OBS record distant arrivals from large earthquakes and local swarms of smaller tremors. These arrivals can be used to provide information relating to the source mechanisms and subsurface structures, if enough stations record the arrivals. An OBS needs to be designed to be able to carry and deploy a heavy and large sensor package with a dynamic range of 0.01 Hz to about 30 Hz, and to operate autonomously for up to one year. Because of the longer deployment durations, a long-lasting internal clock is required with high precision for accurate time stamping of raw data.

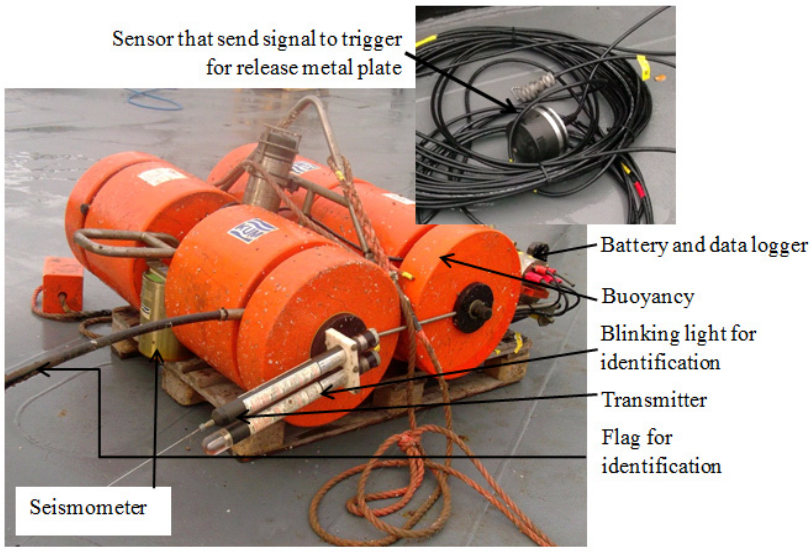

FIGURE 11: Ocean bottom seismometer

The advantage of OBSs for recording on the seabed rather than using towed arrays to record in the water column is that OBSs can record seabed shear waves directly as a vector using three component geophones, thus providing useful additional information for the interpretation process.

The major components of the OBS are shown in Figure 11. The system attaches to a heavy metal plate and is dropped to the sea bottom and

is retrieved after a specific period, most commonly one year. In the retrieval process, a trigger is used to detect the OBS system and a signal is sent to release the system from the attached platform, the metal plate. A buoyancy mechanism activates and the OBS is brought to the surface for safe retrieval.

There are several methods to determine the angle between the sensor north in the OBS and true north. One way is to take known large scale earthquakes within the measuring period and calculate the Rayleigh wave behaviour, enabling us to find the angle between sensor north and true north. Another technique is triggering a blast in a known location at known depth. The wave path of the incoming signals of the controlled source enables us to detect the angle. In the OBS data processing stage, waveforms are rotated by the angle obtained from the above methods.

5.4 Data processing

Several software has been developed to process passive seismic data in real time and post processing approaches. Some are developed with graphical user interfaces (GUI) to process data in an easy manner. In the study of Hellisheidi, a software called SeisComP3 (Seismological Communication Processor) was used, which was originally developed for the GEOFON program, and is maintained by the GEOFON software development group at GFZ Potsdam. This is an open source, freely available software and it consists of acquisition, picking and analysing facilities. The software can be configured to accommodate different projects and site characteristics, in order to locate earthquakes accurately and reliably.

Figure 12 explains the front page view of the software. The map (A) can be used to view the suspected area and enter the initial guess (location of the earthquake and origin time). After entering the initial guess, we can pick P and S waves.

Using the picking tool in the picker window shown in Figure 13, we can pick the P and S wave arrival times for all the stations within a certain distance. Available data are displayed in the bottom of the window. Depending on our objectives, we can apply different filters to enhance the signal. In the case study area, a 4-10 Hz bandpass filter was used. After picking all the stations, the data is sent to the locater and the main window appears. By returning to the main window, different methods and velocity models can be chosen to relocate the earthquake.

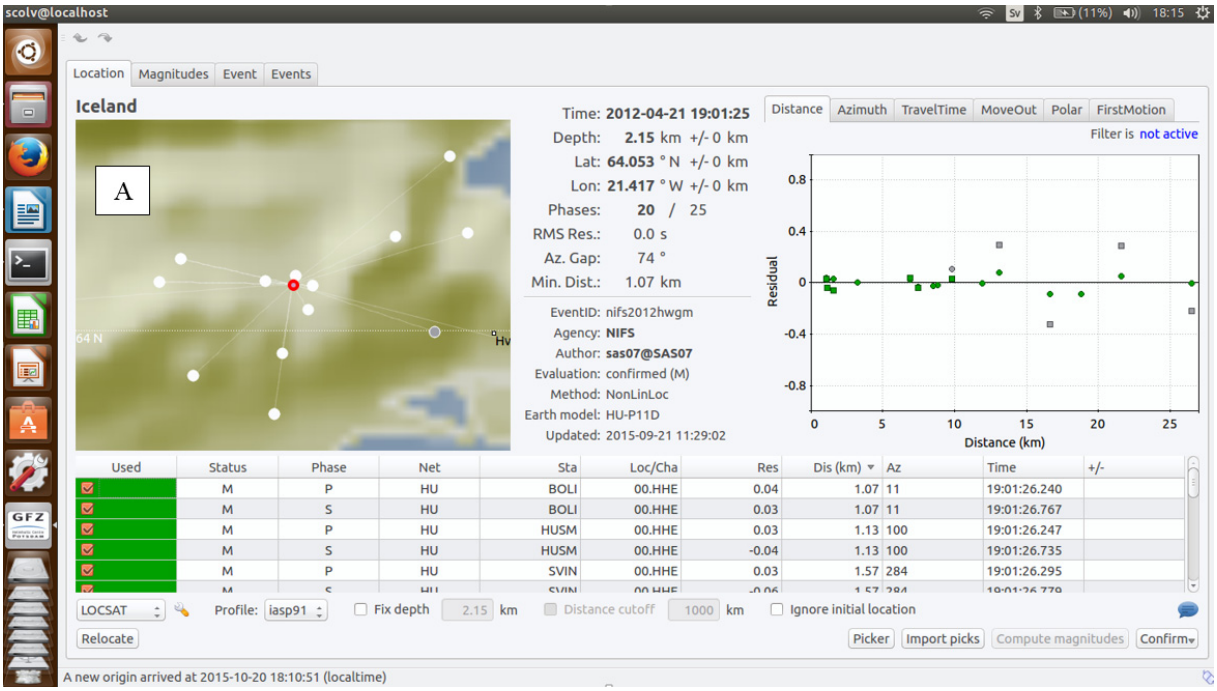

FIGURE 12: Front view of the SeisComP3 software

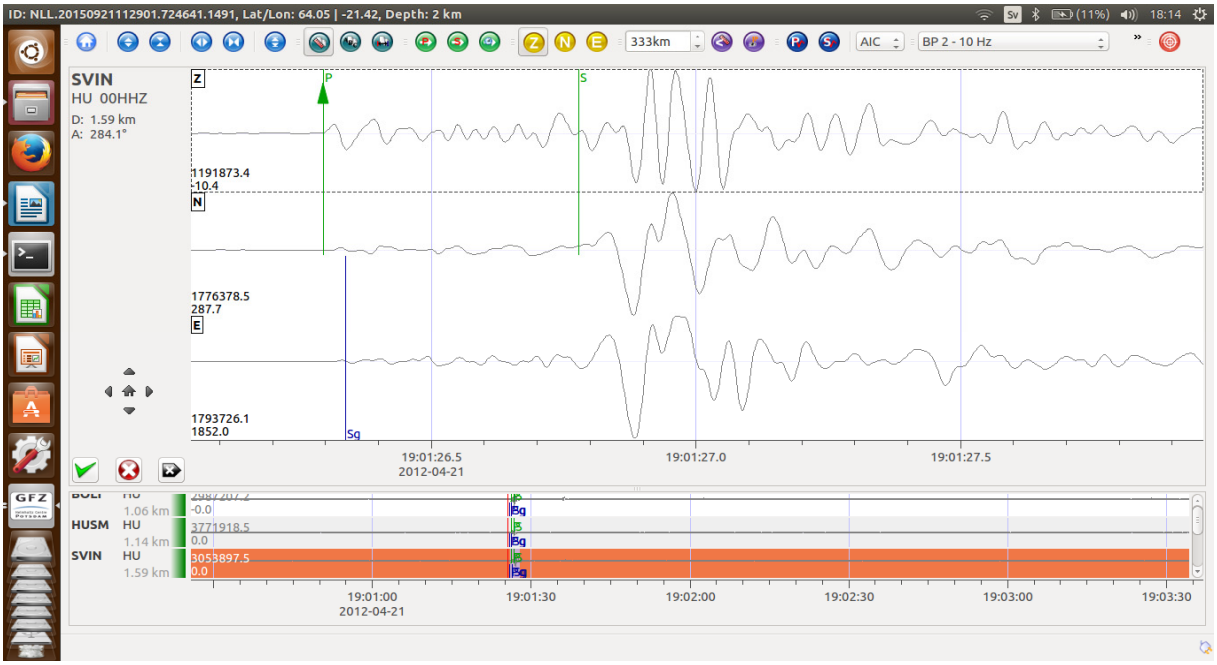

FIGURE 13: Picker window in the SeisComP3 software showing P and S waves from an event in Hellisheidi

5.5 Velocity model

The velocity model is one of the most important parts of processing passive seismic data. The accuracy of the location always depends on the accuracy of that model. Constructing velocity models is not an easy task. Data collected from vertical seismic profiling and drill holes are mainly used to construct the model. Depending on the data gathered, the velocity can be modelled as a 1D, 2D or 3D model. 1D models, in which the velocity changes only in the z direction and is constant in the X and Y directions, is the most available model. 2D and 3D models are more accurate than 1D, but are harder to obtain.

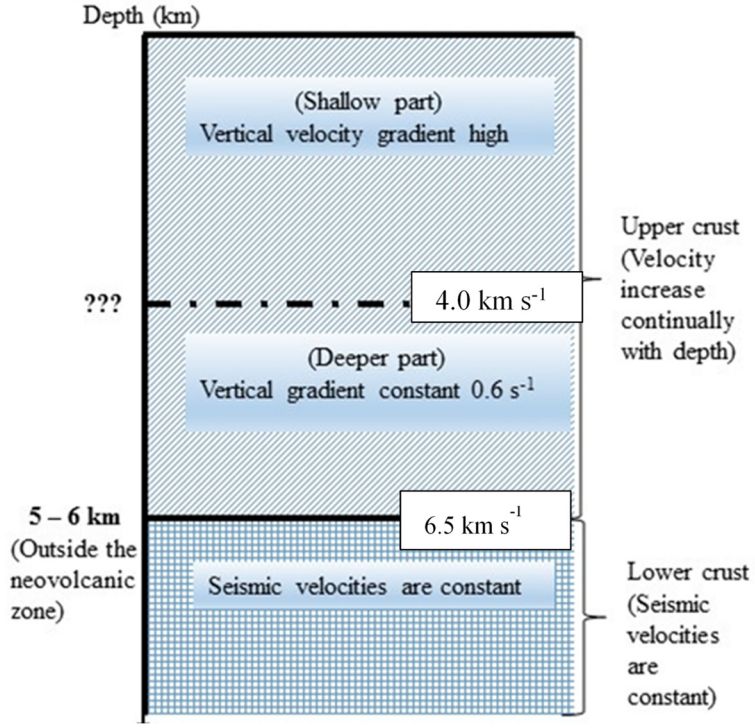

FIGURE 14: Icelandic crustal structure according to Flóvenz (1980)

5.5.1 Average one-dimensional crustal structure of Iceland

The general tomographic inversion of Iceland was done by Flóvenz in 1980 (Foulger and Toomey, 1989) and it represents the general velocity depth structure. In this structure the Icelandic crust is divided into two main divisions, upper crust and lower crust. Details of the velocity model interpretation can be seen in Figure 14. (Foulger and Toomey, 1989)

5.5.2 Velocity of the Hengill triple junction volcanic system

Three major principle high-velocity bodies are recognized in the Hengill area, which correlate with three extinct volcanic systems. These bodies can be explained as dense, intrusive, solidified, shallow crustal magma reservoirs. Grensdalur and Ölkelduháls are still hot and host the geothermal field while Húsmúli is cold.

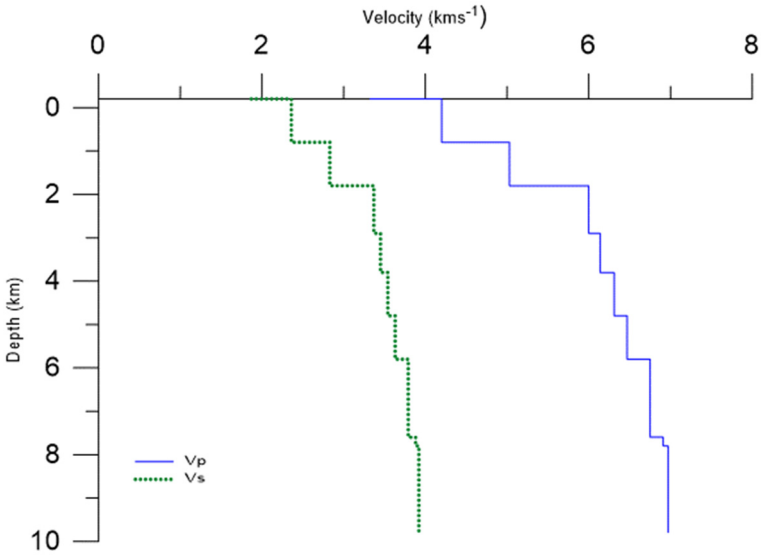

FIGURE 15: Velocity model used to process the Hellisheidi seismic data

The velocity model that we used for the Hellisheidi area is given in Figure 15. The density of the layers are constant in that model at 2.5 kg m^{-3}. P and S wave velocities that have significant difference and velocity changes are very small compared to depth. Locating earthquakes is a non-linear problem and inverse modelling is used to solve the problem. All these features are included in the NonLinLoc procedure, which is available as a plugin for the SeisComP3 software (Lomax, et al., 2015).

6. RESULTS AND DISCUSSION

6.1 Seismic monitoring in Hellisheidi area (Case study)

Waste water from the Hellisheidi power plant is reinjected into the system through wells in Húsmúli. It started in September 2011 and in the period of 2011-2012 a large number of induced earthquake activities were recorded in the area. One of the earthquake swarms recorded in that series was used to demonstrate the processing steps. The seismic events took place in Húsmúli in a two-day period in 2012, from April 21st to April 22nd. It was picked and located with the SeisComP3 software. The events had a magnitude range from -1 to 3, and the evolution of the swarm is shown in Figure 16. It follows a typical earthquake swarm behaviour. The activity started around 17:00 on the 21st April and reached a peak around midnight. After that it slowly decays until it fades out at midnight of 22nd April.

6.1.1 Event distribution and depth variation

Figure 17 shows the depth distribution of the seismic events located in the swarm. It shows that most of the events are in the range of 1.61-2.61 km. Figure 18 shows the seismic event density in map view and Figure 19 shows NS and EW profiles. It clearly shows that the recorded swarm delineates a N-S striking vertically dipping fault.

Figure 20 shows that the seismic events concentrate some distance from the reinjection zone. Figure 21 shows the overall seismic activities in that area in the 2011-2012 period and clearly shows that the activity moves westward with time, away from the injection site. It is one of the most interesting observations in the Húsmúli area.

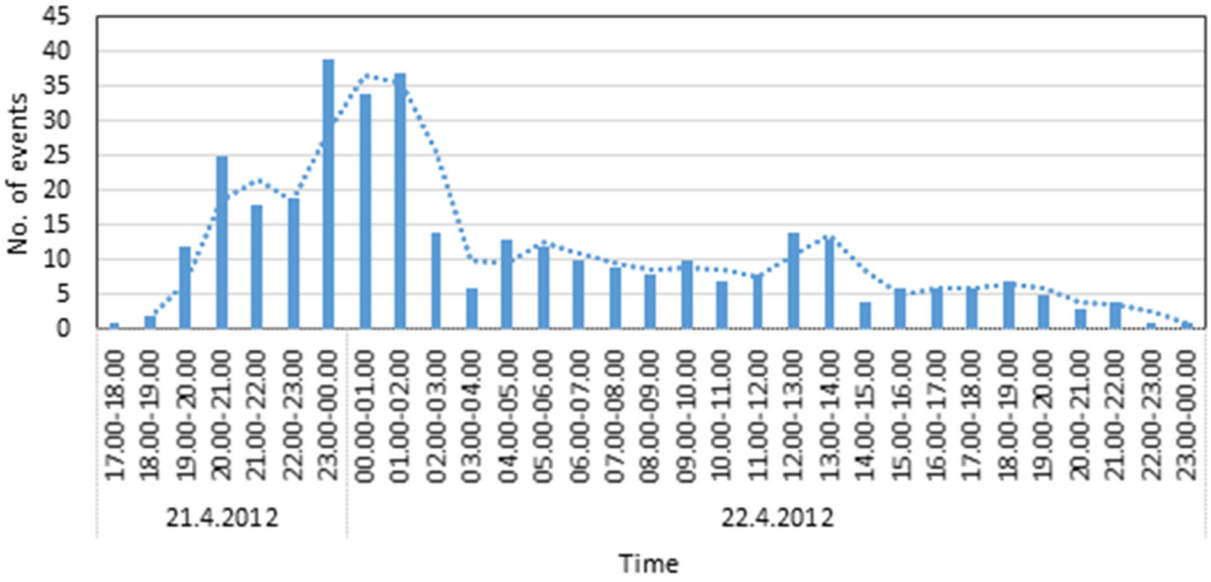

FIGURE 16: Frequency distribution of swarm

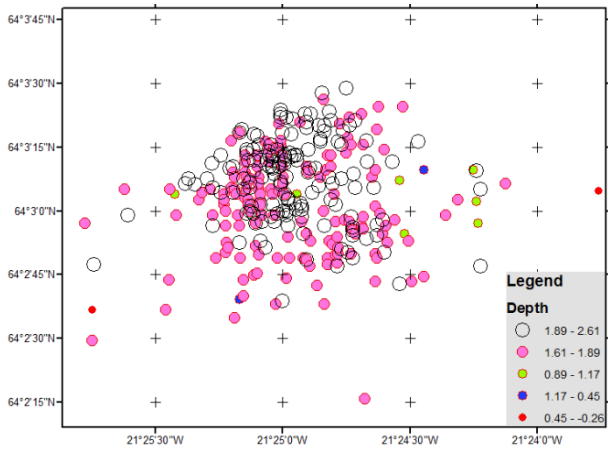

FIGURE 17: Events depth distribution in map view

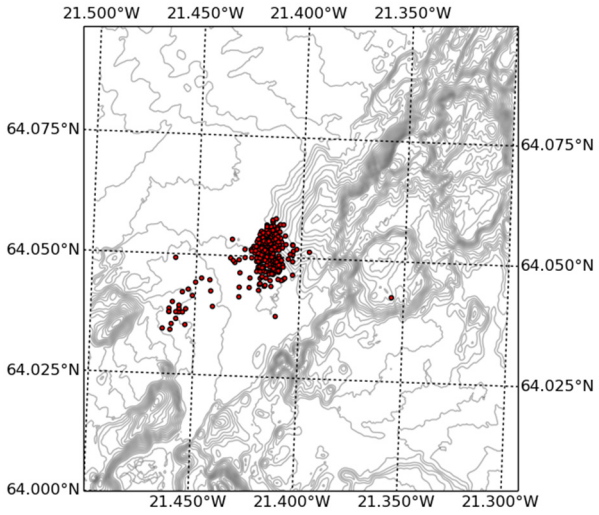

FIGURE 18: Event distribution of the located swarm, 360 earthquake events were located in the range of -1 to 3 M during 2012.04.21 – 2012.04.22

6.2 Review of seismic monitoring in geothermal projects in comparison with case study site

Learning from the mistakes and successes of past geothermal projects allows us to enhance the quality of the monitoring of our own projects. Here, world geothermal case histories will be compared with the Hellisheidi seismic monitoring.

According to environmental laws, geothermal power companies are obliged to reinject waste water back into the aquifer, below the ground water table. With injection comes a high probability of inducing seismic activity in the area. Long term monitoring is very important for identifying both prior and post states of the project area. The Geysers in northern California, USA, is a good case study for this point of view (Majer, 2007) (Figure 22). The area is one of the world's largest geothermal fields and can partly

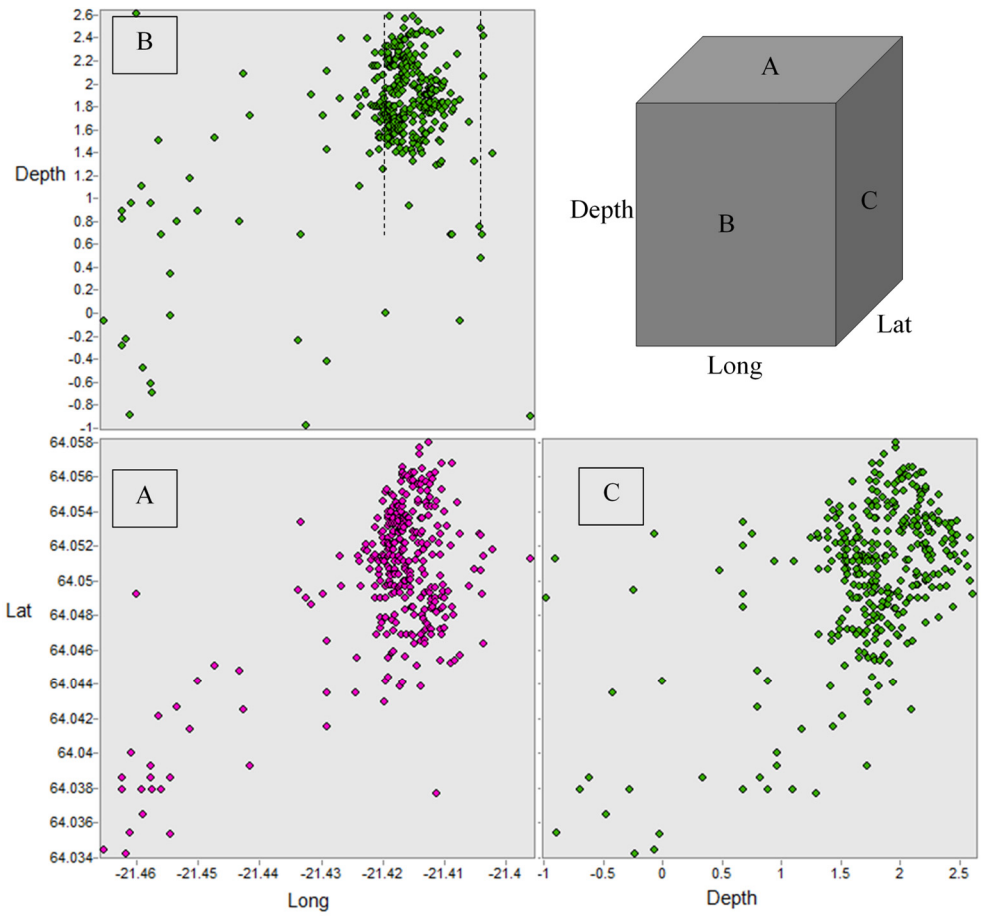

FIGURE 19: Cross-sectional view of the seismic activities; A) shows the seismicity as viewed from above, B) is an E-W cross-section and C) is a N-S cross-section

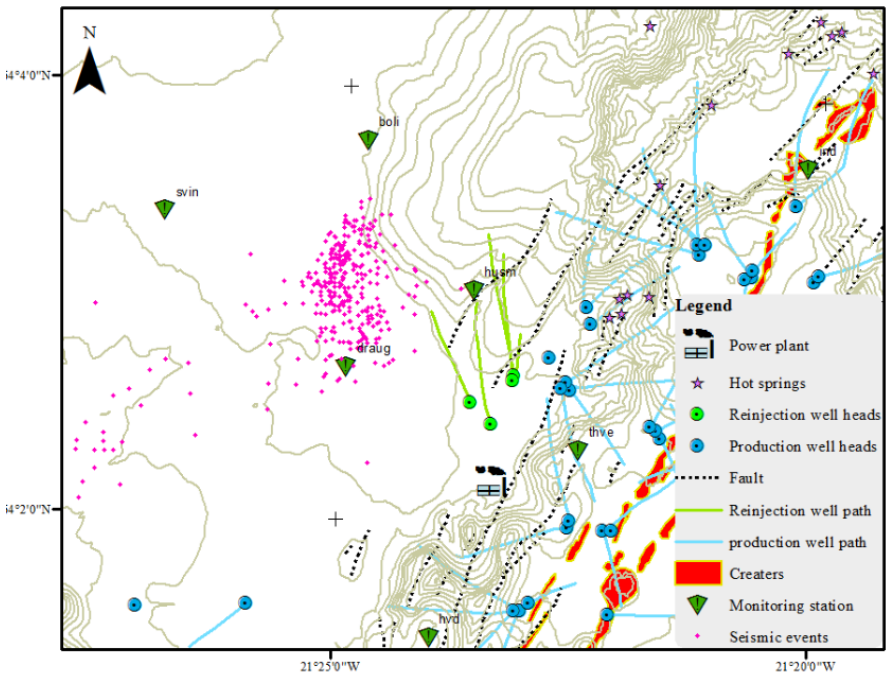

FIGURE 20: Location of the seismic swarm (pink diamonds) in relation with the location of the injection wells (green lines)

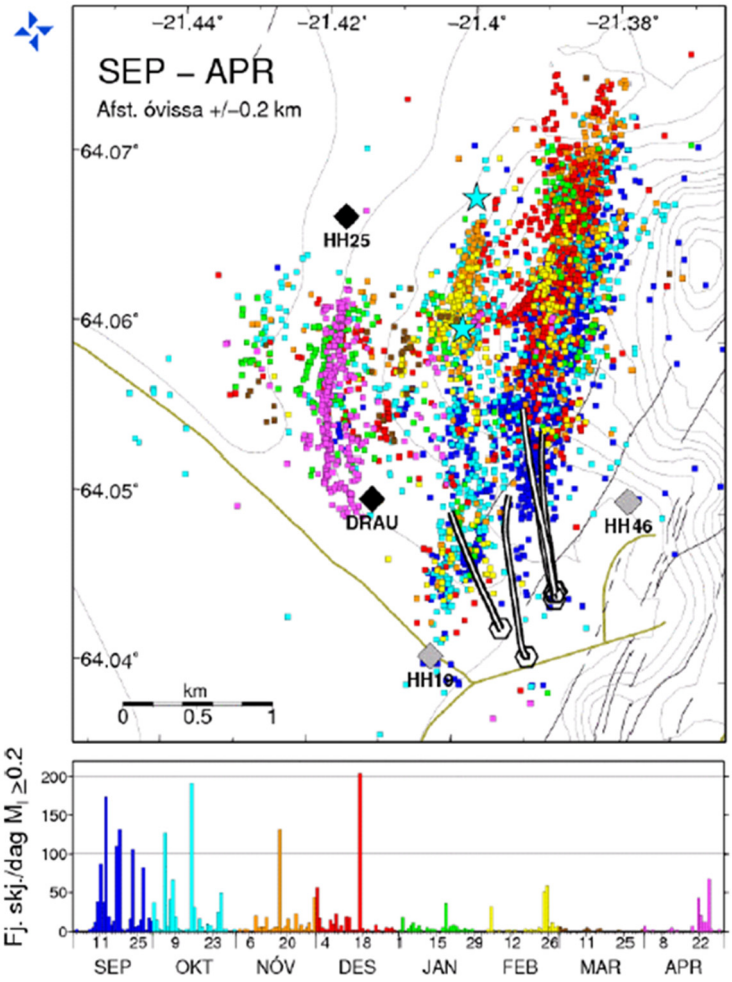

FIGURE 21: Overall seismic activity in the Húsmúli area during 2011-2012 (Bessason, et al. 2012)

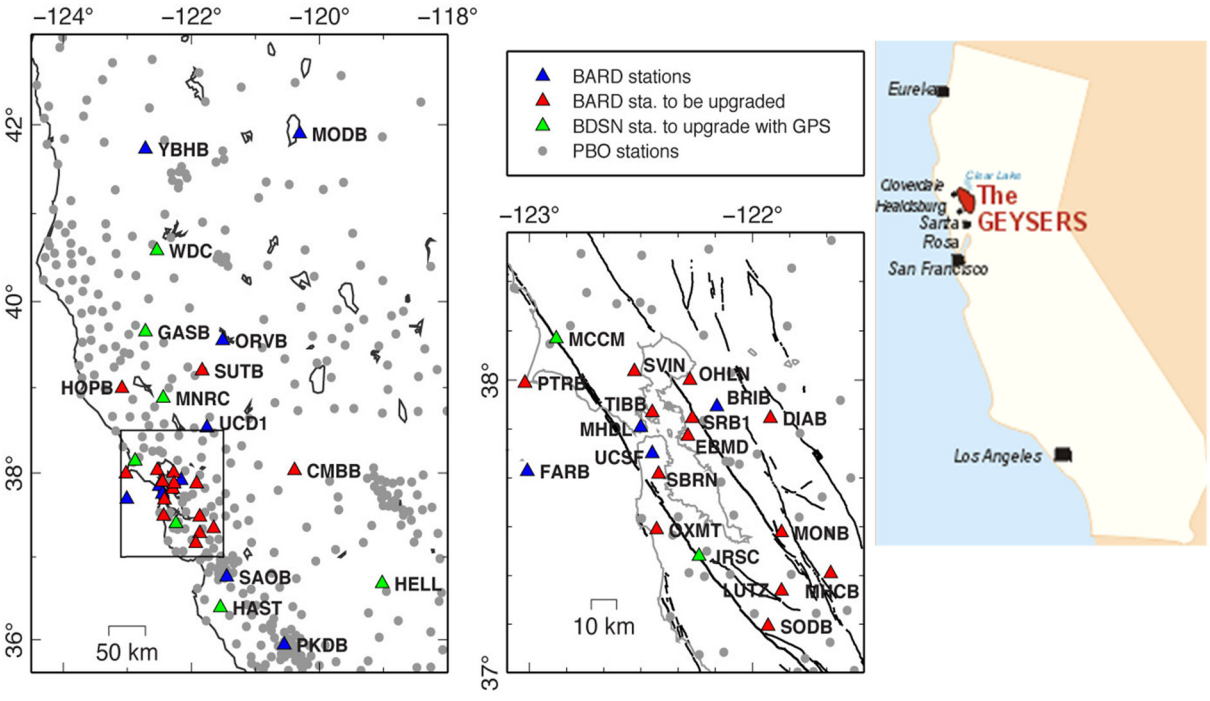

FIGURE 22: Seismic monitoring system related to The Geysers system, USA (BSL, 2015)

be identified as an enhanced geothermal system. As in Hellisheidi, seismic activities have been recorded in relation with mass extraction and reinjection of the geothermal field. The field has been monitored continually for a number of years. The wide coverage of the seismic network, including the injection and production areas, as well as neighbouring areas, has enabled scientists to examine the field-wide response to injection. Currently, the nearest station to Hellisheidi is located nearly 9 km away from the event site. It shows the importance of increasing the number of stations in the network for better evaluation.

When reinjection started in the Cooper Basin field in Australia, the number of earthquakes in the area drastically increased. Fortunately, the project is located in a remote area, minimizing negative effects on local population. There are some benefits to locating geothermal projects close to communities: it reduces the cost of transmitting electricity or opens new avenues for the use of hot water for various purposes. However, strong community oppositions can lead to the termination or postponing of energy projects. Three events larger than M 3.0, induced during the development stages of an enhanced geothermal system in Basel, Switzerland, led to the suspension of the project (Majer, 2007). In the Hellisheidi area, the nearest community lies around 10 km away from the operation area. This is a comparably large distance, but the events with a magnitude larger than M 3.0 could be felt in the community (Bessason et al., 2012).

Careful monitoring of seismic activity is a valuable tool to get a better idea about subsurface activities, which otherwise would go unnoticed.

Controlling risk associated with induced seismicity is the ultimate goal of continuous monitoring. This is twofold. *Reducing the risk of the power project*; thorough research of the subsurface activities reduces the uncertainty of the effects of the mass extraction and reinjection. *Increasing safety;* safety issues are major factors that any project should consider at all stages. Taking precaution strategies against seismic events is important for the operation of the power plant, as well as the neighbouring community. The Berlin, El Salvador, project has a built-in warning system for monitoring, quantifying and controlling the risk associated with induced seismicity (Majer, 2007). When a destructive event takes place, it is very important to identify whether it is an induced event or a natural seismic event for the decision making process. The gap that exists today between acquired knowledge and the real situation needs to be bridged. A field like Berlin, which has a high degree of natural earthquakes, could serve as a test site for further development of mitigation processes. Figure 23 describes the traffic light system that is used in Berlin for maintaining the field. A real time monitoring system is essential for this system and should be located in the injection and production zones.

A detailed description of the traffic light system can be expressed as follows:

Green; ground shaking below the general detectability. Operation proceeds according to plan.
Amber; everyone can feel ground shaking but damages are very unlikely. Injection continues with caution and, depending on the situation, flow rate can be reduced and observations intensified.
Red; lower main boundary (thick line) indicates that events have crossed the safety level. In this stage ground shaking can be experienced and very light damage can be expected. When it crosses the upper minor boundary (dashed line) weak structures may be damaged and injection is suspended immediately. Beyond the upper minor boundary is where high levels of damage are expected.

A risk management plan like this is essential in monitoring of all active sites. In the Hellisheidi geothermal field induced seismicity is controlled by keeping the injection rate steady. The seismic monitoring system could be improved, as was suggested by Bessason et al. (2012). Active communications with the public is a valuable social tool to increase awareness and acceptance of geothermal power projects.

As a final step, filling gaps of existing knowledge is most important for future decisions. Access to funds and data for researchers is imperative to reach this goal. Active participation in the international science community is the key to finding new solutions to dealing with induced seismicity.

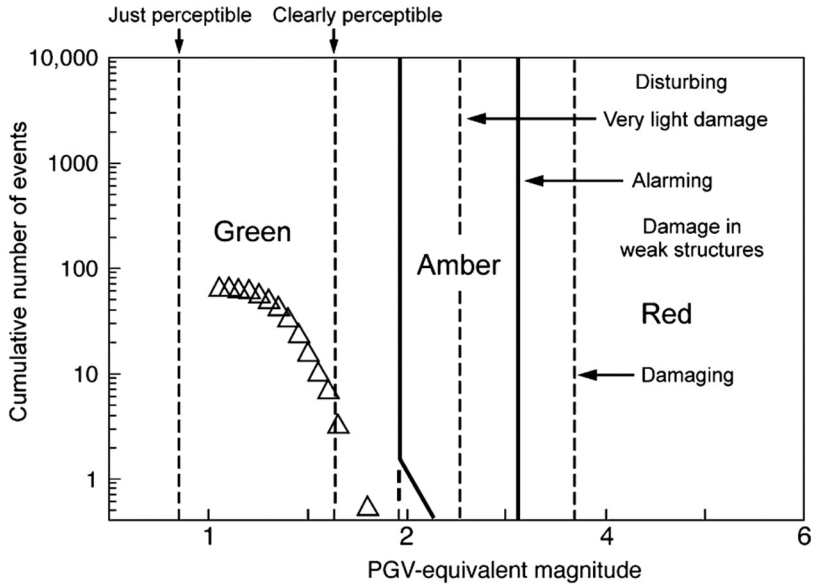

FIGURE 23: "Traffic light" boundaries superimposed on event recurrence defined in terms of magnitudes adjusted to produce the epicentral Peak Ground Velocity (PGV) if their focal depths were exactly 2 km. Triangles represent the cumulative recurrence data from the three episodes of fluid injection (totalling 54 days of pumping) normalized to a period of 30 days in The Geysers, USA. (Majer, 2007)

7. CONCLUSIONS

The ultimate goal of seismic monitoring in geothermal fields is to find the best methodologies to minimize negative impacts of induced seismicity and increase the positive aspects for the sustainable use of resources. A major element of this is close and continuous monitoring of the geothermal field. Following successful methodologies in the initial stages gives more reliable results and helps to make more reliable decisions. A case study was done in Hellisheidi geothermal field, which is one of the monitored geothermal fields in Iceland. One earthquake swarm was analysed and results show that the recorded swarm delineates a N-S trending vertically dipping fault. The swarm was a part of a larger sequence of induced earthquakes taking place in the area in connection with reinjection of geothermal waste water. Detailed study of the overall seismicity has shown that the activity moves to the west with time, away from the injection well. Seismic study is a powerful tool for the monitoring of geothermal fields and having these kinds of observations are invaluable for decision makers.

ACKNOWLEDGEMENTS

I would like to express my gratitude to the Government of Iceland and the United Nations University Geothermal Training Programme for granting me the opportunity to be a fellow in this excellent programme. Special thanks goes to family of UNU-GTP, Director Lúdvík S. Georgsson, Deputy Director Ingimar G. Haraldsson, Ms. Málfrídur Ómarsdóttir, Ms. Thórhildur Ísberg and Mr. Markús A.G. Wilde for their assistance and guidance through these six months. I would also like to acknowledge my supervisor Ms. Sigríður Kristjánsdóttir for her support and patience, helpful discussion and useful advice. I also thank Gylfi Páll Hersir for his guidance and encouragement. ISOR has generously supported me in this work, for which I am very thankful.

Last but not least, I am forever grateful for the effort of my institute (National Institute of Fundamental Studies) in Sri Lanka which was always available for advice and support.

REFERENCES

Bessason, B., Ólafsson, E.H., Gunnarsson, G., Flóvenz, Ó.G., Jakobsdóttir, S.S., Björnsson, S., and Árnadóttir, Th., 2012: *Working procedures due to induced seismicity in geothermal systems*. Reykjavík Energy, Reykjavík, internal report (in Icelandic), 10 pp.

BSL, 2015: *Map of Bay area regional deformation network sites*. University of California, Berkeley Seismological Laboratory, Berkeley, CA, US. Website: *http://seismo.berkeley.edu/ bard/map.html*

Ellsworth, B., 2013: *Injection-induced seismicity.* U.S. Geological Survey, Earthquake Science Center seminars, lecture notes, 75 pp. Website: *http://earthquake.usgs.gov/regional/nca/seminars/2013-12-02/*

Evans, K.F., Zappone, A., Kraft, T., Deichmann, N., and Moia, F., 2011: A survey of the induced seismic responses to fluid injection in geothermal and CO_2 reservoirs in Europe. *Geothermics, 41*, 30-54.

Flóvenz, Ó.G., 1980: Seismic structure of the Icelandic crust above layer three and the relation between body wave velocity and the alteration of the basaltic crust. *J. Geophys. 47,* 211-220.

Foulger, G.R., and Toomey, D.R., 1989: Structure and evolution of the Hengill-Grensdalur volcanic complex, Iceland: Geology, geophysics, and seismic tomography. *J. Geophysical Research: Solid Earth*, *94*, 17511-17522.

Gunnarsson, G., Kristjánsson, B.R., Gunnarsson, I., and Júlíusson, B.M., 2015: Reinjection into a fractured reservoir – induced seismicity and other challenges in operating re-injection wells in the Hellisheidi field, SW-Iceland. *Proceedings of the World Geothermal Congress 2015, Melbourne, Australia*, 9 pp.

Gunnarsson, G., 2013: Temperature dependent injectivity and induced seismicity – managing re-injection in the Hellisheidi field, SW-Iceland. *Geothermal Resources Council, Transactions, 37*, 1019-1025.

Halldórsson, B., Rupakhety, R., and Sigbjörnsson, R., 2012: On the effects of induced earth quakes due to fluid injection at Hellisheidi geothermal power plant, Iceland. *Proceedings of the 15th World Conference on Earthquake Engineering, Lisboa, Portugal*, 10 pp.

LBNL, 2015: *Induced seismicity*. Lawrence Berkeley National Laboratory (LBNL), Berkeley, CA, United States. Website: *http://esd1.lbl.gov/research/projects/ induced_seismicity/primer.html#defined*

Lay, T., and Wallace, T.C., 1995: *Modern global seismology*. Academic Press, San Diego, CA, United States, 521 pp.

Lomax, A.A., Michelini, A.C., and Curtis, A., 2009: Earthquake location, direct, global-search methods. In: Meyers, R.A. (ed.), *Encyclopedia of complexity and system science*. Springer, NY, US, 2449-2473.

Majer, E.L., Baria, R., Stark, M., Oates, S., Bommer, J., Smith, B., and Asanuma, H., 2007: Induced seismicity associated with enhanced geothermal systems. *Geothermics, 36-3*, 185-222.

Nordquist, G., 2005: Microearthquake monitoring and applications. *WPRB/INAGA Bali Seminar 2008, Bali, Indonesia*, 27 pp.

Seale, S., Vincent, H., and NEES EOT, 2011: *Everything important about earthquakes (and other assorted information)*. The George E. Brown Network for Earthquake Engineering Simulation (NEES). Website: *https://nees.org/resources/3936*

APPENDIX I: The temporary seismic networks operated in Reykjanes - Hellisheidi area

Name of station	Latitude	Longitude
GRV	63.8572	-22.4558
KAS	64.0229	-21.8520
KRI	63.8781	-22.0765
NYL	63.9737	-22.7379
RNE	63.8168	-22.7056
VOG	63.9697	-22.3929
VOS	63.8528	-21.7036
BJA	63.9459	-21.3026
HEI	64.1998	-21.2360
KRO	64.0981	-21.1198
KUD	64.3206	-21.8747
SAN	64.0560	-21.5701
SOL	63.9290	-20.9436
HUSM	64.0513	-21.3938
BOLI	64.0626	-21.4133
HIMN	64.0490	-21.3524
THVE	64.0393	-21.3744
DRAUG	64.0451	-21.4158
LYKL	64.0823	-21.5450
SVIN	64.0566	-21.4485
BUG	63.9045	-21.4376
ELB	63.8582	-21.9872
ENG	64.0879	-21.4105
GEI	63.9482	-21.5307
HAH	63.9286	-22.6386
HDV	63.8699	-21.8839
HOV	63.9530	-22.0830
HVD	64.0245	-21.3995
HVV	64.1118	-21.2158
ISS	63.8629	-22.3029
LAG	63.9052	-22.4888
LAT	63.8583	-22.1869
LHL	63.9792	-21.8320
LME	63.9742	-21.4291
LSK	64.0350	-21.2960
MOH	63.9200	-22.0596
NUP	63.9989	-21.2536
SEL	64.1336	-21.2383
SOG	63.9927	-21.1496
STH	63.9863	-22.2652
SVH	63.8779	-21.5515
TRH	64.0608	-21.1798
ASH	63.9871	-22.1361
BIT	64.0573	-21.2577
BLF	63.9737	-21.6489
FAF	63.9064	-22.2148
GUD	64.0198	-21.1885
HRG	63.9606	-21.9779
HVH	64.0097	-21.3356
IND	64.0616	-21.3358
KLV	63.9112	-21.9582
LHA	64.0241	-21.0489
LSF	63.9222	-22.3722
SEA	63.8434	-22.1112
SHR	64.0240	-21.5016
SKD	64.1079	-21.2988
VSV	63.8737	-22.5881

APPENDIX II: Seismic events recording during 21 April – 22 April 2012

Date	Time	Latitude	Longitude	Depth (km)	RMS	d_lat (km)	d_lon (km)	d_dep (km)	M	Picking mode
21.4.2012	00:17:11.405	63.9755	-21.4565	0.8	0.061	0.88	1.58	1.31	1.95	manual
22.4.2012	00:00:10.751	64.0435	-21.4291	-0.42	0.063	2.33	2.42	2.01	1.71	manual
22.4.2012	00:00:17.382	64.0379	-21.4575	-0.69	0.002	1.49	1.66	1.47	1.73	manual
22.4.2012	00:04:07.650	64.0513	-21.396	-0.9	0.009	1.44	1.61	1.42	1.61	manual
22.4.2012	00:05:08.967	64.0455	-21.4241	1.73	0.042	0.52	0.75	0.6	1.22	manual
22.4.2012	00:09:30.012	64.0545	-21.4142	1.95	0.053	0.35	0.34	0.33	1.18	manual
22.4.2012	00:16:37.096	64.0538	-21.419	2.27	0.06	0.22	0.2	0.3	1.33	manual
22.4.2012	00:18:58.644	64.0485	-21.4101	1.84	0.047	0.21	0.25	0.26	1.21	manual
22.4.2012	00:19:23.297	64.0454	-21.4082	1.83	0.029	0.22	0.26	0.27	1.03	manual
22.4.2012	00:20:22.247	64.0471	-21.4132	1.84	0.041	0.46	0.59	0.58	1.17	manual
22.4.2012	00:20:42.945	64.0536	-21.4137	1.79	0.035	0.35	0.35	0.34	1.07	manual
22.4.2012	00:21:25.978	64.0353	-21.4545	-0.02	0.023	0.78	0.92	0.88	0.97	manual
22.4.2012	00:22:01.687	64.0485	-21.4087	0.68	0.042	1.65	1.7	1.56	1.53	manual
22.4.2012	00:22:38.801	64.0557	-21.4129	1.8	0.035	0.63	0.71	0.62	1.1	manual
22.4.2012	00:28:54.953	64.0448	-21.4433	0.8	0.021	1.76	2.01	1.82	1.68	manual
22.4.2012	00:29:54.934	64.0425	-21.4427	2.09	0.007	1.59	2.25	1.07	2.39	manual
22.4.2012	00:33:51.693	64.0494	-21.4126	1.84	0.02	0.26	0.25	0.3	1.06	manual
22.4.2012	00:33:10.526	64.0386	-21.4576	-0.62	0.002	1.5	1.71	1.51	1.73	manual
22.4.2012	00:35:52.173	64.0525	-21.415	2.59	0.057	0.23	0.18	0.32	1.36	manual
22.4.2012	00:37:13.345	64.0551	-21.4195	1.96	0.049	0.25	0.23	0.25	1.07	manual
22.4.2012	00:34:39.365	64.0386	-21.4544	0.34	0.008	1.47	1.67	1.46	1.72	manual
22.4.2012	00:37:35.487	64.0563	-21.4152	2.19	0.039	0.29	0.22	0.36	1.14	manual
22.4.2012	00:35:16.805	64.0527	-21.4138	1.51	0.01	1.47	1.75	1.51	1.69	manual
22.4.2012	00:39:35.802	64.0456	-21.4164	1.78	0.037	0.59	0.82	0.68	1.17	manual
22.4.2012	00:40:09.126	64.04	-21.4609	0.96	0.014	1.57	1.84	1.57	1.64	manual
22.4.2012	00:40:32.358	64.0492	-21.4296	1.72	0.003	1.48	1.77	1.54	1.76	manual
22.4.2012	00:47:48.375	64.0529	-21.4173	2.24	0.043	0.26	0.22	0.35	1.18	manual
22.4.2012	00:49:40.772	64.054	-21.417	2.33	0.052	0.18	0.18	0.27	1.29	manual
22.4.2012	00:50:04.750	64.0496	-21.4122	1.9	0.022	0.19	0.21	0.26	1.15	manual
22.4.2012	00:52:17.680	64.0415	-21.4291	1.43	0.042	0.45	0.68	0.6	1.03	manual
22.4.2012	00:55:14.944	64.0365	-21.459	-0.48	0.005	1.36	1.63	1.42	1.7	manual
22.4.2012	00:55:46.814	64.0354	-21.4611	-0.89	0.015	1.16	1.19	1.46	0.86	manual
22.4.2012	01:03:22.857	64.0522	-21.4108	1.5	0.033	0.23	0.25	0.39	2.33	manual
22.4.2012	00:59:33.738	64.0531	-21.4169	2.41	0.033	0.27	0.26	0.41	1.01	manual
22.4.2012	00:59:55.386	64.0518	-21.423	1.94	0.008	0.63	0.68	0.66	1.01	manual
22.4.2012	01:00:21.193	64.0506	-21.404	0.48	0.013	1.44	1.59	1.4	1.68	manual
22.4.2012	01:01:16.804	64.0492	-21.4039	0.68	0.017	1.45	1.57	1.39	1.56	manual
22.4.2012	01:04:48.339	64.0527	-21.4074	-0.07	0.007	1.52	1.72	1.52	1.72	manual
22.4.2012	01:05:26.341	64.052	-21.409	0.68	0.017	1.54	1.73	1.5	1.92	manual
22.4.2012	01:05:48.811	64.0414	-21.4514	1.17	0.036	1.64	1.92	1.68	1.63	manual
22.4.2012	01:06:27.479	64.0465	-21.429	2.11	0.007	0.85	1.12	0.83	2.45	manual
22.4.2012	01:06:42.872	64.0442	-21.4501	0.89	0.022	1.79	2.06	1.81	1.8	manual
22.4.2012	01:07:19.986	64.0494	-21.4101	1.98	0.038	0.18	0.23	0.25	1.03	manual
22.4.2012	01:09:39.072	64.0511	-21.4197	1.87	0.013	0.88	1.16	0.87	2.18	manual
22.4.2012	01:10:30.618	64.0514	-21.427	1.87	0.003	2.28	2.99	2.11	0.88	manual
22.4.2012	01:13:48.511	64.0471	-21.4182	1.65	0.008	1.53	1.14	1.43	1.7	manual
22.4.2012	01:14:46.681	64.0451	-21.4473	1.53	0.03	1.18	1.65	0.93	2.51	manual
22.4.2012	01:16:12.309	64.0497	-21.4268	2.39	0.004	1.28	2.42	0.93	1.68	manual
22.4.2012	01:18:59.821	64.0532	-21.4095	2.15	0.041	0.25	0.23	0.34	1.05	manual
22.4.2012	01:20:29.692	64.0536	-21.4165	2.05	0.05	0.25	0.2	0.33	1.53	manual
22.4.2012	01:22:41.511	64.0393	-21.4577	0.96	0.003	1.42	1.72	1.48	1.87	manual
22.4.2012	01:24:46.703	64.0545	-21.4078	2.26	0.045	0.27	0.3	0.3	1.27	manual
22.4.2012	01:25:00.006	64.0514	-21.424	1.88	0.027	0.49	0.59	0.42	1.49	manual
22.4.2012	01:25:39.632	64.0533	-21.4165	2.02	0.03	0.23	0.23	0.26	1.42	manual
22.4.2012	01:26:15.656	64.0561	-21.4123	1.83	0.05	0.26	0.28	0.27	1.11	manual
22.4.2012	01:27:13.908	64.0551	-21.4167	2.17	0.069	0.23	0.24	0.27	1.28	manual
22.4.2012	01:27:54.419	64.0492	-21.4601	2.61	0.001	2.54	2.98	2.02	0.88	manual
22.4.2012	01:28:09.465	64.0379	-21.4624	0.89	0.003	1.9	2.45	1.56	2.31	manual
22.4.2012	01:30:35.885	64.0551	-21.4195	1.81	0.05	0.27	0.25	0.31	1.08	manual
22.4.2012	01:31:21.673	64.0386	-21.4624	0.82	0.011	1.48	1.79	1.5	1.79	manual
22.4.2012	01:33:50.233	64.0379	-21.4559	0.68	0.008	1.45	1.69	1.45	1.66	manual

Date	Time	Latitude	Longitude	Depth (km)	RMS	d_lat (km)	d_lon (km)	d_dep (km)	M	Picking mode
22.4.2012	01:35:42.383	64.0558	-21.4155	1.74	0.047	0.42	0.42	0.69	1.19	manual
22.4.2012	01:36:12.585	64.0379	-21.4591	1.1	0.012	1.47	1.7	1.47	1.62	manual
22.4.2012	01:36:52.746	64.0521	-21.4228	1.9	0.033	0.47	0.54	0.39	1.16	manual
22.4.2012	01:42:18.270	64.0486	-21.4316	1.9	0.052	0.6	0.71	0.57	1.03	manual
22.4.2012	01:49:35.434	64.0377	-21.4113	1.29	0.04	0.93	0.5	0.67	1.59	manual
22.4.2012	01:50:12.866	64.0427	-21.4535	0.8	0.03	1.56	2.39	1.04	1.88	manual
22.4.2012	01:51:48.086	64.0497	-21.4236	1.8	0.014	0.55	0.67	0.58	0.94	manual
22.4.2012	01:52:54.938	64.0393	-21.4416	1.72	0.001	1.4	1.53	1.38	1.72	manual
22.4.2012	01:54:45.896	64.0435	-21.4243	1.72	0.025	0.77	0.92	1	0.92	manual
22.4.2012	01:55:23.084	64.0455	-21.4192	1.66	0.05	0.58	0.8	0.69	0.99	manual
22.4.2012	02:07:36.815	64.0546	-21.42	1.8	0.041	0.51	0.58	0.42	2.46	manual
22.4.2012	02:11:53.766	64.0379	-21.4624	-0.28	0.01	1.54	1.83	1.55	1.67	manual
22.4.2012	02:16:32.808	64.0553	-21.4193	2.21	0.042	0.56	0.73	0.6	1.25	manual
22.4.2012	02:19:41.234	64.0527	-21.4106	1.3	0.004	1.51	1.76	1.51	1.74	manual
22.4.2012	02:20:07.228	64.0479	-21.4098	1.8	0.049	0.24	0.3	0.29	1.1	manual
22.4.2012	02:22:48.634	64.0543	-21.4122	1.76	0.065	0.19	0.18	0.27	2.04	manual
22.4.2012	02:24:43.157	64.0485	-21.4153	2.45	0.078	0.21	0.19	0.28	1.29	manual
22.4.2012	02:30:07.096	64.0527	-21.4042	0.75	0.008	1.47	1.69	1.46	1.73	manual
22.4.2012	02:33:42.677	64.0505	-21.4159	2.14	0.042	0.2	0.19	0.25	1.13	manual
22.4.2012	02:34:59.703	64.0563	-21.4115	1.79	0.058	0.23	0.23	0.26	1.16	manual
22.4.2012	02:36:51.954	64.0568	-21.4104	1.83	0.037	0.29	0.33	0.39	1.18	manual
22.4.2012	02:44:37.402	64.0517	-21.4224	2.39	0.073	0.33	0.39	0.36	1.27	manual
22.4.2012	02:48:30.139	64.0558	-21.4151	1.98	0.061	0.22	0.21	0.26	1.21	manual
22.4.2012	02:50:55.959	64.048	-21.4136	1.71	0.033	0.22	0.2	0.24	1.27	manual
22.4.2012	03:00:44.670	64.0543	-21.4174	1.96	0.037	0.28	0.24	0.37	1.26	manual
22.4.2012	03:36:35.796	64.0543	-21.4128	1.9	0.05	0.58	0.93	0.55	1.33	manual
22.4.2012	03:47:50.721	64.0535	-21.4161	2.03	0.034	0.34	0.38	0.32	1.07	manual
22.4.2012	03:55:09.478	64.0504	-21.4173	2.28	0.061	0.19	0.19	0.28	2.24	manual
22.4.2012	03:49:15.852	64.0496	-21.4114	1.79	0.03	0.25	0.26	0.3	1.09	manual
22.4.2012	03:57:13.788	64.0505	-21.4155	2.43	0.06	0.25	0.28	0.31	1.25	manual
22.4.2012	04:00:13.168	64.05	-21.4188	2.59	0.014	0.68	0.79	0.68	0.91	manual
22.4.2012	04:03:37.498	64.0344	-21.4653	-0.07	0.017	1.47	1.79	1.49	1.74	manual
22.4.2012	04:04:49.525	64.0342	-21.4616	-0.23	0.019	1.06	1.3	1.01	0.98	manual
22.4.2012	04:04:57.091	64.049	-21.4212	2.15	0.052	0.27	0.26	0.25	1.15	manual
22.4.2012	04:19:58.207	64.0504	-21.4132	2.32	0.01	1.01	1.31	1.1	1.54	manual
22.4.2012	04:22:57.340	64.0514	-21.4037	2.42	0.036	0.77	1.24	0.9	1.66	manual
22.4.2012	04:24:20.929	64.0421	-21.4563	1.51	0.001	1.5	1.81	1.55	1.85	manual
22.4.2012	04:36:17.601	64.0556	-21.4123	1.95	0.06	0.19	0.22	0.27	1.42	manual
22.4.2012	04:39:25.035	64.0487	-21.4121	2.05	0.038	0.41	0.64	0.34	1.21	manual
22.4.2012	04:49:33.743	64.0568	-21.4088	1.76	0.033	0.33	0.34	0.41	1.19	manual
22.4.2012	04:53:39.953	64.0546	-21.4112	1.94	0.029	0.5	0.86	0.91	1.13	manual
22.4.2012	04:57:20.732	64.0556	-21.4143	2.1	0.038	0.19	0.21	0.26	1.62	manual
22.4.2012	04:59:06.814	64.0552	-21.4127	2.03	0.033	0.21	0.22	0.27	1.21	manual
22.4.2012	05:06:44.867	64.0501	-21.4158	2.22	0.035	0.21	0.23	0.25	1.16	manual
22.4.2012	05:06:11.574	64.0559	-21.4119	2.02	0.032	0.25	0.29	0.3	1.21	manual
22.4.2012	05:02:05.915	64.0507	-21.4181	1.66	0.012	0.71	0.46	0.83	2.55	manual
22.4.2012	05:07:35.817	64.0504	-21.4181	2.15	0.025	0.64	0.41	0.42	3.43	manual
22.4.2012	05:09:48.370	64.0503	-21.4154	2.21	0.052	0.17	0.17	0.18	1.35	manual
22.4.2012	05:25:37.595	64.0498	-21.417	2.14	0.051	0.17	0.15	0.17	1.15	manual
22.4.2012	05:26:55.491	64.0498	-21.419	2.15	0.054	0.19	0.16	0.19	1.22	manual
22.4.2012	05:27:48.574	64.0501	-21.4154	2.24	0.057	0.2	0.19	0.19	1.44	manual
22.4.2012	05:34:25.030	64.0536	-21.4207	2.15	0.017	0.6	0.61	0.81	2.67	manual
22.4.2012	05:34:50.285	64.05	-21.4166	2.22	0.054	0.19	0.15	0.18	1.21	manual
22.4.2012	05:42:04.737	64.0473	-21.4204	1.81	0.032	0.29	0.31	0.35	1	manual
22.4.2012	05:53:16.032	64.0517	-21.4168	2.22	0.051	0.4	0.23	0.25	1.05	manual
22.4.2012	06:08:00.690	64.0522	-21.4166	1.7	0.011	0.46	0.67	0.92	2.51	manual
22.4.2012	06:09:29.373	64.0522	-21.418	2.36	0.027	0.19	0.19	0.18	1	manual
22.4.2012	06:36:48.914	64.0504	-21.4189	1.77	0.005	0.39	0.64	0.81	1.74	manual
22.4.2012	06:42:13.924	64.0518	-21.4134	2.25	0.013	0.29	0.72	0.4	0.88	manual
22.4.2012	06:30:07.036	64.0472	-21.413	1.56	0.01	0.29	0.41	0.82	2.52	manual
22.4.2012	06:37:16.451	64.0525	-21.4199	1.25	0.04	0.97	0.93	1.04	2.37	manual
22.4.2012	06:43:22.034	64.0504	-21.4205	1.8	0.01	0.37	0.38	0.77	2.63	manual
22.4.2012	06:54:53.869	64.0513	-21.4169	1.72	0.04	0.41	0.61	0.77	2.45	manual

Date	Time	Latitude	Longitude	Depth (km)	RMS	d_lat (km)	d_lon (km)	d_dep (km)	M	Picking mode
22.4.2012	06:51:22.227	64.0442	-21.4195	0	0.02	0.9	1.08	0.91	2.47	manual
22.4.2012	07:16:42.131	64.0476	-21.4202	1.73	0.033	0.41	0.7	0.6	1.92	manual
22.4.2012	06:59:59.653	64.049	-21.4139	2.08	0.027	0.6	0.59	0.92	2.38	manual
22.4.2012	07:18:40.202	64.0507	-21.4181	1.63	0.012	0.36	0.54	0.82	2.53	manual
22.4.2012	07:09:40.265	64.0504	-21.4181	1.56	0.005	0.76	0.75	0.9	2.19	manual
22.4.2012	07:22:36.701	64.0503	-21.4106	1.81	0.046	0.17	0.18	0.17	1.17	manual
22.4.2012	07:24:58.700	64.0553	-21.4105	1.77	0.01	0.4	0.39	0.6	2.43	manual
22.4.2012	07:26:39.603	64.0452	-21.409	1.91	0.038	0.15	0.19	0.19	1.09	manual
22.4.2012	07:30:29.866	64.0497	-21.4172	1.7	0.024	0.38	0.64	0.5	2.59	manual
22.4.2012	07:42:27.506	64.0536	-21.4183	1.8	0.006	0.58	1.24	0.95	2.58	manual
22.4.2012	07:52:09.565	64.0495	-21.4337	-0.24	0.017	1.55	1.89	1.71	2.47	manual
22.4.2012	08:02:39.751	64.0473	-21.41	2.02	0.035	0.17	0.18	0.19	1.14	manual
22.4.2012	08:20:18.642	64.0483	-21.4131	1.56	0.01	0.31	0.42	0.78	2.52	manual
22.4.2012	08:26:05.952	64.0472	-21.4122	1.6	0.016	0.29	0.43	0.83	2.38	manual
22.4.2012	08:34:50.960	64.0554	-21.4151	2.21	0.044	0.16	0.15	0.17	1.11	manual
22.4.2012	08:45:32.232	64.0525	-21.4191	1.66	0.009	0.57	1.19	0.94	2.41	manual
22.4.2012	08:49:22.623	64.0529	-21.4151	1.56	0.01	0.37	0.37	0.71	2.66	manual
22.4.2012	08:52:23.175	64.0488	-21.4114	1.85	0.038	0.16	0.16	0.17	1.27	manual
22.4.2012	08:57:25.571	64.0498	-21.4103	1.61	0.061	0.15	0.17	0.15	1.63	manual
22.4.2012	09:02:53.455	64.0464	-21.4037	2.06	0.007	1.97	1.71	1.48	2.45	manual
22.4.2012	09:04:31.320	64.0522	-21.4142	1.46	0.015	0.35	0.36	0.71	2.57	manual
22.4.2012	09:04:52.282	64.0525	-21.415	1.53	0.018	0.38	0.47	0.81	2.7	manual
22.4.2012	09:05:32.125	64.0525	-21.415	1.32	0.012	0.34	0.46	0.81	2.53	manual
22.4.2012	09:20:32.668	64.0525	-21.415	1.39	0.018	0.36	0.39	0.74	2.68	manual
22.4.2012	09:24:45.083	64.0511	-21.4157	0.94	0.033	0.46	0.38	1	2.62	manual
22.4.2012	09:32:58.675	64.0469	-21.4105	1.32	0.029	0.27	0.38	0.87	2.47	manual
22.4.2012	09:40:10.096	64.0532	-21.4191	1.49	0.04	0.44	0.45	0.84	2.54	manual
22.4.2012	09:53:44.505	64.049	-21.4195	1.6	0.007	0.33	0.38	0.82	2.53	manual
22.4.2012	09:50:11.786	64.0439	-21.4139	1.41	0.004	1.33	0.97	1.33	2.31	manual
22.4.2012	10:03:31.993	64.0444	-21.4192	1.77	0.007	0.72	1.17	1.14	1.75	manual
22.4.2012	10:04:11.395	64.0469	-21.4137	1.42	0.007	0.28	0.37	0.84	2.48	manual
22.4.2012	10:10:55.801	64.0458	-21.4185	1.7	0.014	0.3	0.41	0.83	2.52	manual
22.4.2012	10:11:45.588	64.0511	-21.4237	1.11	0.024	0.35	0.38	0.89	2.35	manual
22.4.2012	10:12:07.471	64.049	-21.4324	-0.98	0.025	0.35	0.77	1.04	2.61	manual
22.4.2012	10:20:26.825	64.0543	-21.4168	1.49	0.023	0.4	0.33	0.67	2.63	manual
22.4.2012	10:53:11.324	64.0533	-21.4177	2.05	0.024	0.44	0.48	0.45	2.42	manual
22.4.2012	11:16:00.572	64.0469	-21.4121	1.97	0.045	0.17	0.2	0.21	1.2	manual
22.4.2012	11:24:38.658	64.0522	-21.419	1.56	0.016	0.39	0.47	0.82	2.34	manual
22.4.2012	11:26:43.859	64.0529	-21.4183	1.8	0.017	0.32	0.36	0.44	2.58	manual
22.4.2012	11:35:57.493	64.043	-21.4198	1.73	0.027	0.39	1.12	1.17	2.47	manual
22.4.2012	11:40:45.056	64.0522	-21.4182	1.6	0.008	0.55	0.51	0.88	2.52	manual
22.4.2012	11:42:19.509	64.0511	-21.4181	1.6	0.031	0.39	0.35	0.73	2.47	manual
22.4.2012	11:49:19.525	64.0514	-21.4198	1.53	0.015	0.37	0.36	0.81	2.49	manual
22.4.2012	11:55:31.180	64.0549	-21.4183	2.17	0.062	0.24	0.24	0.25	1.14	manual
22.4.2012	12:02:20.078	64.0507	-21.4221	1.39	0.004	1.78	1.99	1.78	2.51	manual
22.4.2012	12:14:17.730	64.0561	-21.4164	2.05	0.052	0.25	0.19	0.19	1.1	manual
22.4.2012	12:18:06.294	64.0559	-21.4135	2.02	0.048	0.18	0.15	0.17	1.31	manual
22.4.2012	12:21:29.221	64.0536	-21.4175	1.9	0.015	0.47	0.51	0.76	2.59	manual
22.4.2012	12:18:53.235	64.0479	-21.4203	1.84	0.024	0.35	0.66	0.66	2.73	manual
22.4.2012	12:23:34.463	64.0547	-21.4142	2.17	0.047	0.23	0.3	0.26	2.17	manual
22.4.2012	12:31:09.450	64.0561	-21.4168	2.14	0.038	0.19	0.19	0.19	1.17	manual
22.4.2012	12:33:03.849	64.0565	-21.4136	2.03	0.056	0.22	0.19	0.19	1.13	manual
22.4.2012	12:34:20.547	64.0539	-21.4176	1.49	0.016	0.38	0.35	0.7	2.63	manual
22.4.2012	12:36:17.007	64.056	-21.416	2.07	0.061	0.16	0.15	0.15	1.21	manual
22.4.2012	12:51:21.034	64.0475	-21.4128	1.9	0.068	0.17	0.19	0.18	1.32	manual
22.4.2012	12:48:57.794	64.0539	-21.4176	1.94	0.017	1.66	1.2	1.88	2.41	manual
22.4.2012	12:57:29.877	64.0563	-21.4148	2	0.04	0.22	0.18	0.18	2.39	manual
22.4.2012	12:49:18.197	64.0518	-21.4166	1.63	0.033	0.48	0.74	0.9	2.38	manual
22.4.2012	13:10:00.165	64.0514	-21.419	1.63	0.011	0.45	0.53	0.86	2.52	manual
22.4.2012	13:01:38.308	64.0514	-21.4182	1.7	0.016	0.37	0.55	0.8	2.49	manual
22.4.2012	13:13:17.146	64.0469	-21.4153	1.42	0.022	0.43	0.52	1.02	2.66	manual
22.4.2012	13:23:19.971	64.0514	-21.4182	1.49	0.004	0.36	0.36	0.76	2.41	manual
22.4.2012	13:03:32.329	64.0536	-21.4191	1.46	0.024	0.4	0.43	0.82	2.31	manual

Date	Time	Latitude	Longitude	Depth (km)	RMS	d_lat (km)	d_lon (km)	d_dep (km)	M	Picking mode
22.4.2012	13:14:33.943	64.0536	-21.4167	1.39	0.037	0.39	0.39	0.72	2.51	manual
22.4.2012	13:19:56.750	64.0529	-21.4135	1.39	0.008	0.51	0.41	0.95	2.45	manual
22.4.2012	13:28:35.008	64.0478	-21.4134	1.51	0.011	0.37	0.53	0.9	2.4	manual
22.4.2012	13:36:28.799	64.0468	-21.4151	1.48	0.026	0.21	0.3	0.29	2.32	manual
22.4.2012	13:43:36.745	64.0457	-21.4074	1.86	0.085	0.16	0.17	0.18	1.73	manual
22.4.2012	13:47:28.270	64.0468	-21.4151	1.98	0.035	0.27	0.33	0.36	2.49	manual
22.4.2012	13:57:01.874	64.0466	-21.4131	1.79	0.014	0.38	0.47	0.47	1.89	manual
22.4.2012	13:58:25.105	64.0451	-21.4144	1.53	0.008	0.26	0.41	0.88	2.07	manual
22.4.2012	14:15:05.882	64.048	-21.4148	1.81	0.037	0.17	0.17	0.19	1.15	manual
22.4.2012	14:26:59.925	64.0515	-21.4212	2.27	0.035	0.31	0.25	0.25	2.65	manual
22.4.2012	14:50:40.139	64.0511	-21.4133	1.66	0.008	0.35	0.4	0.72	2.76	manual
22.4.2012	14:57:59.536	64.049	-21.4099	1.63	0.015	0.35	0.65	0.57	2.51	manual
22.4.2012	15:01:58.050	64.0543	-21.4176	1.6	0.026	0.41	0.35	0.66	2.6	manual
22.4.2012	15:16:04.767	64.0545	-21.4178	1.4	0.019	0.38	0.34	0.71	2.75	manual
22.4.2012	15:18:28.918	64.0566	-21.4168	2.07	0.078	0.19	0.17	0.17	1.22	manual
22.4.2012	15:24:32.321	64.0557	-21.4169	1.6	0.003	0.79	0.73	0.92	2.5	manual
22.4.2012	15:25:45.079	64.0543	-21.4182	2.15	0.031	0.18	0.16	0.18	1.19	manual
22.4.2012	15:37:08.974	64.0529	-21.4167	1.56	0.024	0.39	0.34	0.69	2.69	manual
22.4.2012	15:49:15.174	64.0573	-21.414	1.86	0.045	0.19	0.17	0.16	1.11	manual
22.4.2012	15:56:50.085	64.0577	-21.4141	1.96	0.043	0.22	0.18	0.18	1.15	manual
22.4.2012	16:19:05.334	64.0533	-21.4185	2.41	0.041	0.22	0.21	0.21	1.29	manual
22.4.2012	16:21:55.546	64.054	-21.419	2.33	0.031	0.23	0.18	0.2	1.02	manual
22.4.2012	16:31:52.455	64.058	-21.4125	1.96	0.045	0.27	0.31	0.23	1.02	manual
22.4.2012	16:34:12.474	64.0459	-21.4183	1.66	0.041	0.28	0.45	0.46	1.05	manual
22.4.2012	16:41:04.486	64.0534	-21.4332	0.68	0.008	1.44	1.87	1.43	1.76	manual
22.4.2012	16:42:14.211	64.0496	-21.4154	2.34	0.061	0.16	0.17	0.17	1.87	manual
22.4.2012	17:02:23.959	64.0541	-21.4172	1.44	0.033	0.4	0.4	0.69	2.66	manual
22.4.2012	17:30:16.840	64.0492	-21.4184	1.58	0.008	0.53	0.42	0.88	2.56	manual
22.4.2012	17:34:41.847	64.0473	-21.4124	1.93	0.055	0.18	0.19	0.19	1.2	manual
22.4.2012	17:36:29.302	64.0487	-21.4121	1.74	0.02	0.28	0.4	0.39	2.43	manual
22.4.2012	17:46:33.938	64.0439	-21.4171	1.82	0.025	0.44	0.41	0.56	2.53	manual
22.4.2012	17:59:10.006	64.0485	-21.4119	1.78	0.016	1.83	1.29	1.11	2.5	manual
22.4.2012	18:11:20.370	64.0508	-21.4191	1.81	0.027	0.35	0.43	0.5	2.7	manual
22.4.2012	18:12:32.371	64.05	-21.4204	1.53	0.031	0.65	0.9	0.95	2.58	manual
22.4.2012	18:29:03.429	64.0441	-21.4167	1.94	0.027	0.41	0.38	0.46	2.57	manual
22.4.2012	18:32:45.225	64.0476	-21.4178	2.21	0.027	0.52	0.78	1.02	2.61	manual
22.4.2012	18:39:10.182	64.0522	-21.4198	1.77	0.002	0.68	1.33	1.01	1.75	manual
22.4.2012	18:40:44.213	64.0529	-21.4199	1.9	0.007	0.56	0.54	0.82	2.62	manual
22.4.2012	18:49:47.901	64.0518	-21.4021	1.39	0.029	1.98	1.67	1.63	2.31	manual
22.4.2012	19:02:35.848	64.055	-21.4185	2.32	0.029	0.2	0.18	0.18	2.48	manual
22.4.2012	19:04:59.700	64.0531	-21.4213	2.03	0.023	0.35	0.41	0.43	2.61	manual
22.4.2012	19:12:35.031	64.0472	-21.4106	1.49	0.016	0.33	0.7	0.97	2.4	manual
22.4.2012	19:44:53.121	64.0454	-21.4106	1.79	0.044	0.21	0.26	0.27	1.25	manual
22.4.2012	19:51:33.698	64.0536	-21.4207	2.15	0.025	0.38	0.74	0.44	1.83	manual
22.4.2012	20:28:42.808	64.0515	-21.4188	1.95	0.035	0.21	0.2	0.21	1.21	manual
22.4.2012	20:40:51.415	64.0469	-21.4162	1.42	0.021	0.33	0.67	1.02	2.54	manual
22.4.2012	21:14:09.577	64.0566	-21.4168	2.1	0.05	0.21	0.16	0.17	1.22	manual
22.4.2012	21:15:36.712	64.0563	-21.4168	2.17	0.055	0.17	0.16	0.16	1.28	manual
22.4.2012	21:16:31.777	64.0525	-21.4191	1.63	0.014	0.39	0.54	0.8	2.69	manual
22.4.2012	20:41:15.650	64.0507	-21.4052	1.32	0.038	0.41	0.43	0.82	2.39	manual
22.4.2012	21:18:49.135	64.048	-21.4084	1.78	0.043	0.15	0.2	0.17	1.4	manual
22.4.2012	22:51:33.509	64.0425	-21.3559	-0.24	0.007	1.25	1.64	1.26	1.77	manual
22.4.2012	23:22:04.832	64.0464	-21.4131	1.9	0.046	0.16	0.18	0.18	1.25	manual
21.4.2012	22:59:11.807	64.0552	-21.4139	2.03	0.054	0.19	0.17	0.16	2.12	manual
21.4.2012	23:29:03.038	64.0532	-21.4175	1.63	0.013	0.39	0.36	0.7	2.45	manual
21.4.2012	23:30:28.728	64.0507	-21.4205	1.56	0.008	0.38	0.54	0.89	2.36	manual
21.4.2012	23:30:36.994	64.0464	-21.4149	1.72	0.007	1.79	2.07	1.82	2.46	manual
21.4.2012	23:30:54.330	64.0479	-21.4195	2.32	0.053	0.68	0.61	0.88	2.71	manual
21.4.2012	23:31:06.387	64.0493	-21.4132	1.77	0.049	0.18	0.23	0.19	1.26	manual
21.4.2012	23:33:16.175	64.0532	-21.4111	2.11	0.068	0.2	0.19	0.19	1.48	manual
21.4.2012	23:35:15.798	64.0469	-21.417	1.63	0.034	0.36	0.36	0.38	1.13	manual
21.4.2012	23:36:44.461	64.0511	-21.4165	1.77	0.034	0.38	0.36	0.75	2.74	manual
21.4.2012	23:41:37.929	64.0529	-21.4151	1.66	0.018	0.6	0.45	0.94	2.47	manual

Date	Time	Latitude	Longitude	Depth (km)	RMS	d_lat (km)	d_lon (km)	d_dep (km)	M	Picking mode
21.4.2012	23:39:19.333	64.0476	-21.413	1.49	0.016	0.3	0.37	0.83	2.58	manual
21.4.2012	23:44:11.232	64.054	-21.41	1.72	0.054	0.17	0.15	0.14	1.69	manual
21.4.2012	23:45:03.713	64.0484	-21.4121	1.95	0.036	0.18	0.17	0.19	1.38	manual
21.4.2012	23:46:42.852	64.0503	-21.4187	2.14	0.051	0.17	0.15	0.19	1.37	manual
21.4.2012	23:47:25.671	64.0493	-21.4123	1.77	0.004	2.54	1.47	2.03	2.74	manual
21.4.2012	23:48:14.810	64.0514	-21.4214	1.8	0.038	0.29	0.29	0.31	1.72	manual
21.4.2012	23:53:03.895	64.0528	-21.4145	2.43	0.048	0.18	0.19	0.16	1.27	manual
21.4.2012	23:54:30.250	64.0485	-21.4151	1.85	0.047	0.22	0.2	0.25	1.14	manual
21.4.2012	23:57:01.086	64.0511	-21.4181	1.7	0.007	0.41	0.5	0.83	2.62	manual
21.4.2012	23:57:53.063	64.0471	-21.4182	1.72	0.006	0.37	0.68	1.03	2.67	manual
21.4.2012	23:58:06.941	64.0536	-21.4135	1.6	0.006	0.53	0.43	0.91	2.73	manual
21.4.2012	23:00:57.823	64.0545	-21.413	1.9	0.032	0.18	0.16	0.16	1.32	manual
21.4.2012	23:02:29.945	64.0489	-21.4121	1.91	0.045	0.17	0.17	0.17	1.39	manual
21.4.2012	23:03:53.785	64.0491	-21.4105	2	0.036	0.16	0.17	0.17	1.96	manual
21.4.2012	23:05:12.553	64.0554	-21.4151	2.14	0.05	0.26	0.21	0.21	1.15	manual
21.4.2012	23:06:17.066	64.0533	-21.4189	2.14	0.056	0.24	0.23	0.24	1.19	manual
21.4.2012	23:06:35.378	64.0518	-21.4182	1.77	0.01	0.37	0.37	0.71	2.68	manual
21.4.2012	23:07:50.754	64.0518	-21.4166	1.56	0.01	0.36	0.37	0.73	2.51	manual
21.4.2012	23:09:07.745	64.0546	-21.4168	1.73	0.024	0.41	0.35	0.67	2.72	manual
21.4.2012	23:10:25.279	64.0483	-21.4163	1.7	0.009	0.32	0.39	0.78	2.64	manual
21.4.2012	23:13:38.756	64.0494	-21.4093	1.84	0.042	0.15	0.16	0.16	1.67	manual
21.4.2012	23:14:59.083	64.0493	-21.4154	1.78	0.02	0.24	0.31	0.32	2.39	manual
21.4.2012	23:18:29.576	64.0522	-21.4136	2.46	0.072	0.19	0.17	0.15	1.35	manual
21.4.2012	23:26:27.402	64.0548	-21.4124	1.85	0.068	0.18	0.17	0.15	1.34	manual
21.4.2012	22:36:40.340	64.0515	-21.4119	1.95	0.066	0.19	0.18	0.24	3.62	manual
21.4.2012	22:38:00.501	64.0511	-21.4165	1.73	0.014	0.36	0.4	0.72	5.11	manual
21.4.2012	22:41:26.248	64.0511	-21.4197	1.53	0.009	0.35	0.36	0.78	2.66	manual
21.4.2012	22:40:29.377	64.0514	-21.4182	1.73	0.008	0.36	0.38	0.71	2.87	manual
21.4.2012	22:45:20.210	64.0529	-21.4169	2	0.024	0.21	0.18	0.19	1.21	manual
21.4.2012	22:47:21.825	64.0482	-21.4112	2.03	0.041	0.16	0.17	0.17	2.27	manual
21.4.2012	22:55:27.018	64.0507	-21.4135	2.05	0.041	0.19	0.16	0.18	1.26	manual
21.4.2012	19:08:16.131	64.048	-21.4181	1.98	0.034	0.2	0.22	0.24	1.28	manual
21.4.2012	18:59:11.941	64.0536	-21.4159	2.28	0.068	0.2	0.18	0.17	1.54	manual
21.4.2012	18:59:35.714	64.0528	-21.4201	2.27	0.046	0.22	0.19	0.2	1.64	manual
21.4.2012	19:01:25.516	64.0531	-21.4169	2.15	0.043	0.24	0.16	0.18	1.51	manual
21.4.2012	19:04:24.962	64.0512	-21.4147	2.26	0.056	0.17	0.18	0.17	1.92	manual
21.4.2012	19:06:46.228	64.0528	-21.4145	2.14	0.068	0.19	0.16	0.18	1.71	manual
21.4.2012	19:10:39.627	64.0528	-21.4149	2.43	0.05	0.17	0.18	0.15	1.97	manual
21.4.2012	19:17:01.348	64.0498	-21.4186	2.14	0.043	0.18	0.17	0.21	1.3	manual
21.4.2012	19:26:14.012	64.0508	-21.4163	2.57	0.03	0.33	0.39	0.42	2.66	manual
21.4.2012	19:30:37.337	64.0512	-21.4199	2.07	0.029	0.3	0.39	0.35	2.3	manual
21.4.2012	19:34:17.942	64.05	-21.4188	1.77	0.01	0.35	0.4	0.77	2.68	manual
21.4.2012	19:37:43.933	64.055	-21.4161	2.18	0.056	0.2	0.15	0.18	1.93	manual
21.4.2012	19:46:28.573	64.0519	-21.4188	2.21	0.033	0.29	0.2	0.22	1.22	manual
21.4.2012	19:47:16.211	64.0519	-21.4168	2.09	0.043	0.18	0.19	0.19	1.81	manual
21.4.2012	19:50:44.831	64.0529	-21.4175	2.01	0.028	0.25	0.33	0.3	1.84	manual
21.4.2012	19:48:56.707	64.0469	-21.421	1.8	0.031	0.28	0.44	0.44	1.3	manual
21.4.2012	19:55:51.920	64.0521	-21.4192	2.19	0.04	0.21	0.18	0.19	1.39	manual
21.4.2012	20:00:46.370	64.0507	-21.4189	1.63	0.016	1.15	1.59	1.3	2.49	manual
21.4.2012	20:02:02.968	64.0522	-21.4164	2.22	0.042	0.35	0.39	0.42	2.75	manual
21.4.2012	20:03:27.575	64.0526	-21.4185	2.17	0.048	0.25	0.25	0.25	1.2	manual
21.4.2012	20:07:23.305	64.0515	-21.4107	2.46	0.044	0.19	0.2	0.16	1.22	manual
21.4.2012	20:11:57.615	64.0512	-21.4207	2.05	0.028	0.28	0.3	0.32	2.44	manual
21.4.2012	20:13:06.621	64.0514	-21.4192	2.24	0.026	0.24	0.24	0.25	1.19	manual
21.4.2012	20:16:08.507	64.0533	-21.4181	2.21	0.035	0.23	0.22	0.24	1.16	manual
21.4.2012	20:16:28.417	64.054	-21.415	2.09	0.032	0.2	0.19	0.18	1.2	manual
21.4.2012	20:22:33.017	64.0511	-21.4205	1.42	0.014	0.35	0.35	0.81	2.64	manual
21.4.2012	20:08:25.863	64.0514	-21.4174	1.66	0.015	0.37	0.57	0.78	2.53	manual
21.4.2012	20:23:58.275	64.0496	-21.4174	2.27	0.042	0.2	0.17	0.18	1.18	manual
21.4.2012	20:25:12.599	64.0492	-21.4184	1.92	0.003	1.92	1.17	1.83	2.36	manual
21.4.2012	20:25:44.248	64.0524	-21.4172	2.38	0.037	0.21	0.21	0.2	1.72	manual
21.4.2012	20:30:42.246	64.0526	-21.404	2.48	0.042	0.23	0.29	0.24	1.23	manual
21.4.2012	20:31:15.164	64.0497	-21.406	1.66	0.016	0.32	0.43	0.69	2.53	manual

Date	Time	Latitude	Longitude	Depth (km)	RMS	d_lat (km)	d_lon (km)	d_dep (km)	M	Picking mode
21.4.2012	20:33:08.788	64.0504	-21.4181	1.66	0.008	0.35	0.37	0.77	2.53	manual
21.4.2012	20:34:37.022	64.0528	-21.4173	2.02	0.028	0.24	0.22	0.24	1.07	manual
21.4.2012	20:38:16.661	64.0477	-21.4184	1.78	0.029	0.37	0.52	0.51	2.32	manual
21.4.2012	20:39:57.876	64.0556	-21.4139	1.9	0.072	0.25	0.18	0.19	1.32	manual
21.4.2012	20:41:15.937	64.0521	-21.4188	1.81	0.019	0.32	0.3	0.33	1.03	manual
21.4.2012	20:42:43.944	64.0535	-21.4165	2.48	0.051	0.27	0.24	0.23	1.27	manual
21.4.2012	20:48:06.118	64.0504	-21.4189	1.7	0.017	0.36	0.57	0.83	2.43	manual
21.4.2012	20:49:28.608	64.0538	-21.4162	2.22	0.042	0.19	0.17	0.18	1.17	manual
21.4.2012	20:58:44.179	64.0511	-21.4173	1.6	0.01	0.36	0.38	0.77	2.62	manual
21.4.2012	20:59:09.918	64.0535	-21.4173	2.33	0.061	0.17	0.15	0.16	1.44	manual
21.4.2012	21:01:27.417	64.0518	-21.4182	1.56	0.011	0.35	0.36	0.74	2.58	manual
21.4.2012	21:09:28.999	64.054	-21.4186	2.14	0.043	0.19	0.15	0.17	1.26	manual
21.4.2012	21:11:11.952	64.0497	-21.4164	2.11	0.04	0.4	0.39	0.6	2.64	manual
21.4.2012	21:13:21.243	64.0524	-21.412	2.43	0.055	0.28	0.24	0.23	1.18	manual
21.4.2012	21:15:43.010	64.0515	-21.42	1.69	0.032	0.33	0.34	0.47	2.72	manual
21.4.2012	21:17:02.763	64.0507	-21.4163	2.38	0.043	0.23	0.22	0.22	1.25	manual
21.4.2012	21:21:37.443	64.0536	-21.4157	2.22	0.066	0.25	0.27	0.26	1.28	manual
21.4.2012	21:30:48.484	64.0518	-21.419	1.53	0.009	0.41	0.5	0.84	2.59	manual
21.4.2012	21:31:08.254	64.0497	-21.4212	1.7	0.006	0.42	1	1.1	2.56	manual
21.4.2012	21:35:36.605	64.0511	-21.4181	1.56	0.012	0.39	0.53	0.85	2.68	manual
21.4.2012	21:36:11.477	64.0507	-21.4205	1.53	0.015	0.42	0.52	0.9	2.7	manual
21.4.2012	21:41:03.002	64.0497	-21.418	1.8	0.01	0.93	1.26	1.28	2.56	manual
21.4.2012	21:42:07.145	64.049	-21.4115	1.66	0.005	0.36	0.96	1.01	2.84	manual
21.4.2012	21:42:53.390	64.0511	-21.4165	2.49	0.053	0.39	0.41	0.43	2.21	manual
21.4.2012	21:43:49.646	64.0535	-21.4165	2.12	0.056	0.19	0.16	0.18	1.32	manual
21.4.2012	21:46:13.969	64.0469	-21.4194	1.7	0.011	0.36	0.5	0.88	2.41	manual
21.4.2012	21:52:00.242	64.0533	-21.4165	2.38	0.062	0.17	0.16	0.16	1.77	manual
21.4.2012	21:56:02.714	64.0533	-21.4181	2.33	0.055	0.19	0.17	0.18	1.28	manual
21.4.2012	22:00:35.767	64.0521	-21.4128	2.45	0.05	0.19	0.19	0.16	1.61	manual
21.4.2012	22:01:04.792	64.0516	-21.4143	2.54	0.051	0.17	0.16	0.15	1.73	manual
21.4.2012	22:02:08.413	64.049	-21.4163	2.21	0.045	0.4	0.26	0.24	1.59	manual
21.4.2012	22:03:55.246	64.0493	-21.418	1.9	0.018	0.43	0.51	0.83	2.56	manual
21.4.2012	22:05:48.816	64.049	-21.4204	1.66	0.014	0.38	0.45	0.85	2.67	manual
21.4.2012	22:05:17.703	64.0497	-21.4196	1.73	0.013	1.06	1.48	1.28	2.57	manual
21.4.2012	22:08:26.533	64.0521	-21.4216	2.15	0.036	0.34	0.36	0.37	2.33	manual
21.4.2012	22:08:59.090	64.0531	-21.4165	2.24	0.035	0.28	0.29	0.28	1.91	manual
21.4.2012	22:09:05.044	64.0512	-21.4219	1.81	0.032	0.32	0.32	0.41	3.65	manual
21.4.2012	22:20:39.027	64.05	-21.414	1.8	0.009	0.35	0.4	0.7	2.52	manual
21.4.2012	22:27:26.902	64.0533	-21.4157	2.43	0.059	0.17	0.18	0.15	1.3	manual
21.4.2012	22:22:36.668	64.0504	-21.4189	1.63	0.013	0.35	0.39	0.77	2.54	manual
21.4.2012	17:17:58.550	64.05	-21.4164	2.01	0.012	0.43	0.72	0.94	2.44	manual
21.4.2012	23:34:21.582	64.0493	-21.4172	1.97	0.011	0.35	0.4	0.73	2.48	manual
21.4.2012	23:51:35.127	64.0465	-21.4137	1.42	0.02	0.35	0.46	0.96	2.58	manual
21.4.2012	22:59:38.053	64.0543	-21.4114	1.81	0.024	0.33	0.2	0.2	3.23	manual
21.4.2012	23:00:10.961	64.0538	-21.4125	1.74	0.022	0.29	0.35	0.28	2.89	manual
21.4.2012	23:11:24.318	64.0514	-21.4174	1.63	0.013	0.41	0.46	0.82	2.62	manual
21.4.2012	23:20:01.232	64.0484	-21.4105	1.96	0.064	0.16	0.16	0.17	1.63	manual